examined the expression profiles of *Dicer* and *eIF2C1~4* during the myogenic differentiation of C2C12 cells and compared them with those of skeletal muscle examined above. As shown in Fig. 3, the expression profiles reveal that the level of expression of either *Dicer* or *eIF2C1~3* is gradually decreased during the myogenic differentiation of C2C12 cells, and that the *eIF2C4* gene is expressed at a low level in either C2C12 myoblast or myotube.

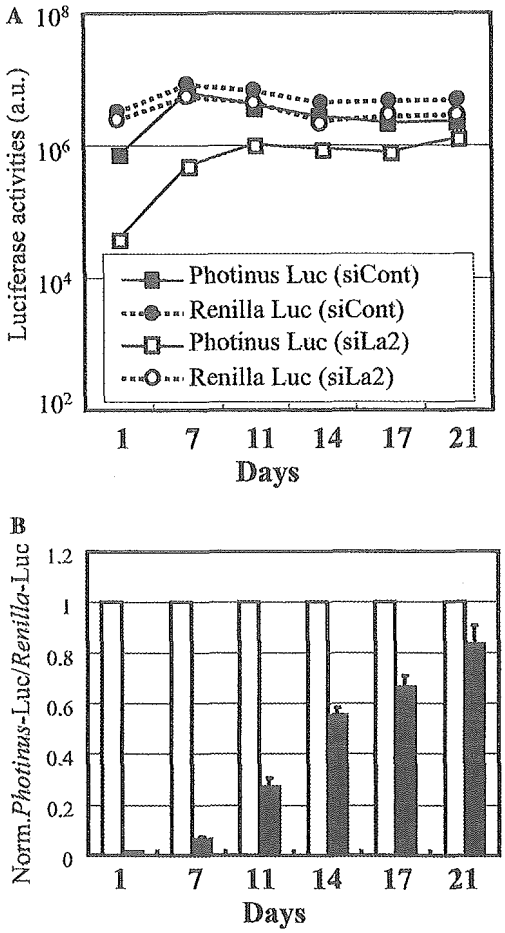

Fig. 4. Persistence of RNAi activity during myogenic differentiation of mouse C2C12 cells. The La2 siRNA duplex or a non-silencing siRNA duplex (Qiagen) together with pGL3-control and pRL-SV40 plasmids were cotransfected into C2C12 cells as in Fig. 2. Before transfection, the culture medium (DMEM containing 15% fetal calf serum) was replaced with DMEM containing 5% horse serum for induction of the myogenic differentiation of C2C12 cells. RNAi activity was examined 24 h after transfection (day 1), and thereafter examined at various days (indicated) up to 3 weeks after the transfection. (A) Absolute *Photinus* and *Renilla* luciferase expressions. The expression levels are plotted in arbitrary luminescence units (a.u.). (B) Ratios of normalised target to control luciferase. Ratios of normalised target (*Photinus*) luciferase activity to control (*Renilla*) luciferase activity are indicated as in Fig. 2. Open and solid bars indicate the data in the presence of the non-silencing siRNA and La2 siRNA duplexes, respectively. Data are averages of at least three independent experiments. Error bars represent standard deviations.

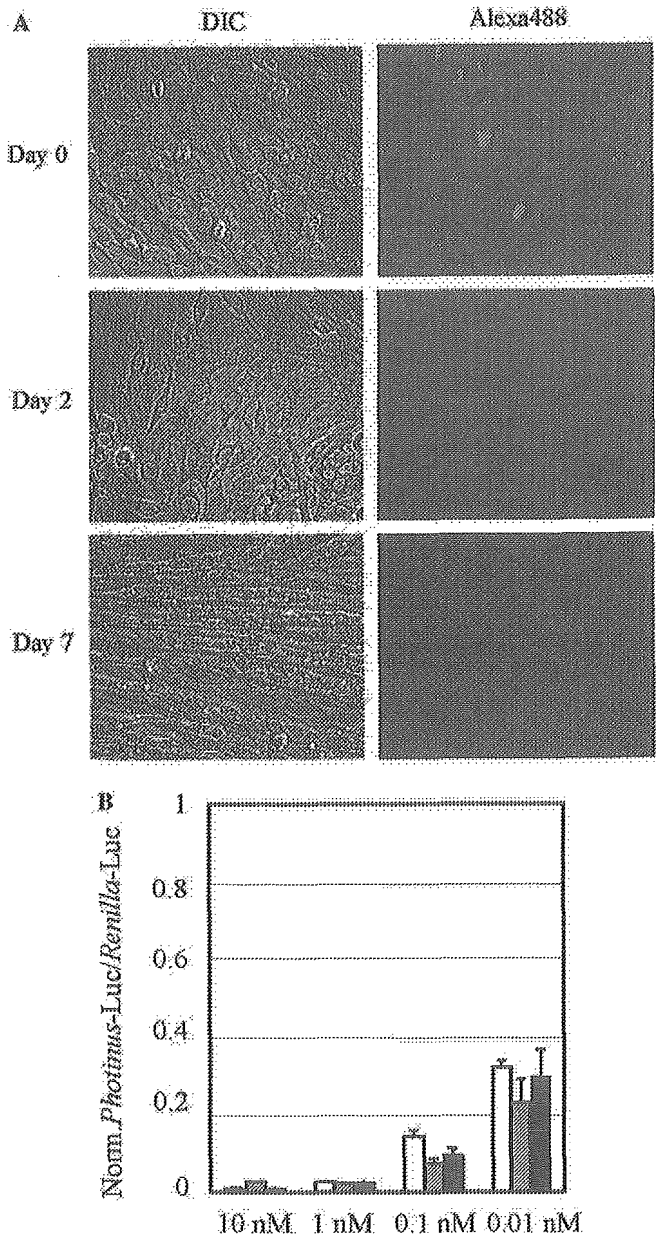

Fig. 5. Cell-cycle arrest and RNAi activity during myogenic differentiation of C2C12 cells. Myogenic differentiation of C2C12 cells was induced by changing the culture medium from DMEM containing 15% fetal calf serum to DMEM containing 5% horse serum. (A) Cell-cycle arrested C2C12 cells. Metabolically labeling of the cells with BrdU was carried out at indicated days after the differentiation. Day 0 indicates undifferentiated C2C12 cells. BrdU incorporated into the cells was visualised with an anti-BrdU antibody and an Alexa488 conjugated secondary antibody. The cells were examined by a florescent microscope. Left (DIC, differential interference contrast) and right (Alexa488, florescence image) panels are identical in visual field. (B) RNAi activity during the differentiation. The reporter plasmids carrying the *Photinus* and *Renilla luciferase* genes were cotransfected with a decreasing amount of the La2 siRNA or non-silencing siRNA duplexes (Qiagen), from 10 to 0.01 nM, into either undifferentiated or differentiated C2C12 cells. Ratios of normalised target (*Photinus*) luciferase activity to control (*Renilla*) luciferase activity are indicated as in Fig. 2. Open, dotted, and solid bars indicate the data in C2C12 cells that differentiated for 0 (undifferentiated), 2, and 7 days, respectively. Data are averages of at least three independent experiments. Error bars represent standard deviations.

Next we examined RNAi activity during the myogenic differentiation of C2C12 cells. The La2 siRNA duplex together with pGL3-control and pRL-SV40 plasmids was cotransfected into undifferentiated C2C12 cells, and simultaneously myogenic differentiation of the cells was carried out by changing culture medium as described above (see Materials and methods). As a result, a strong RNAi activity was detected by day 7 after RNAi induction (Fig. 4), when morphological changes of C2C12 cells into myotubes appeared to be completed (Fig. 5A); thereafter, the cells gradually lost the RNAi activity and lost most of the activity by day 21 after the induction (Fig. 4).

Because proliferating mammalian cells gradually lose RNAi activity with an increase in the number of cell divisions [12,28,29], we investigated whether cell division occurred in C2C12 cells during the differentiation by means of a BrdU incorporation assay. As shown in Fig. 5A, while the incorporation of BrdU into nuclei could be observed in undifferentiated C2C12 cells, few or no BrdU-positive cells were detectable at day 2 and 7 after induction of the differentiation. In addition, from the data of Fig. 5B, the nature of RNAi activity during the differentiation appears to remain unchanged. Consequently, these observations suggest that C2C12 cells differentiated over 2 days are probably cell-cycle arrested cells, and thus that the decrease in RNAi activity during the myogenic differentiation of C2C12 cells is not caused by cell division.

We further examined RNAi activities in C2C12 myotubes that differentiated for 14 and 21 days. The results indicate that RNAi activities induced by synthetic siRNA duplexes are detectable in those differentiated C2C12 myotubes (Fig. 6), although the transfection efficiency of siRNA and plasmid DNA into the cells seemed to become lower as the culture was long. Taking all the data together, it is conceivable that the decrease in RNAi activity during the myogenic

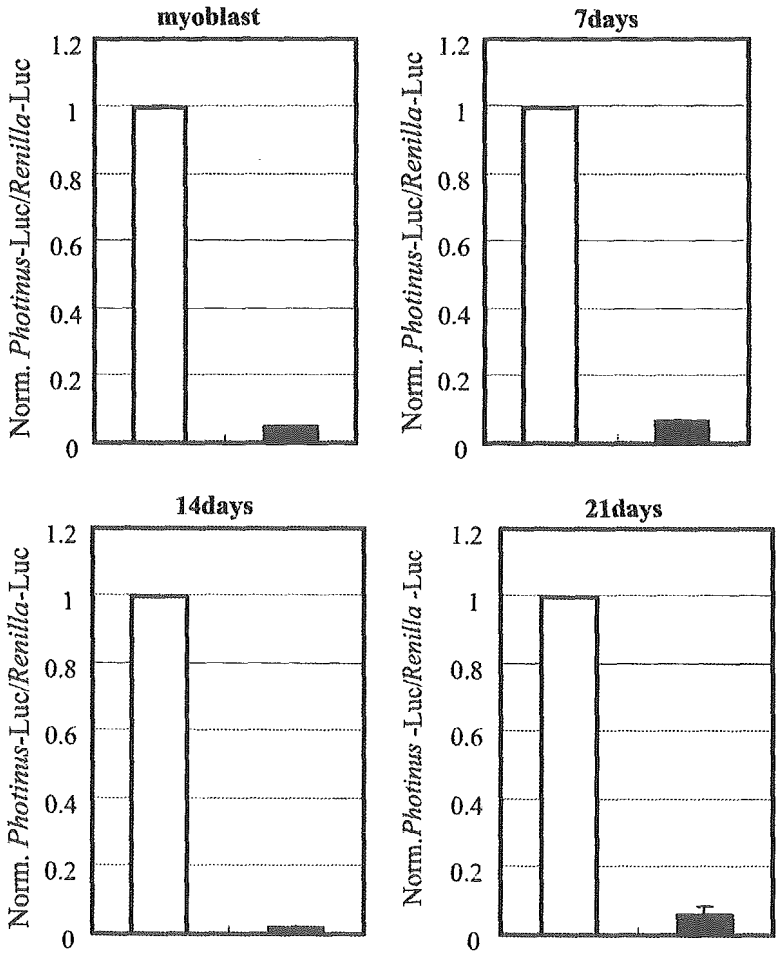

Fig. 6. RNAi induction after myogenic differentiation of C2C12 cells. Myogenic differentiation of C2C12 cells was performed as in Fig. 5. RNAi induction was carried out as in Fig. 2 at indicated days after induction of the myogenic differentiation, and each RNAi activity was examined 24 h after RNAi induction. Ratios of normalised target (*Photinus*) luciferase activity to control (*Renilla*) luciferase activity are indicated as in Fig. 2. Open and solid bars indicate the data in the presence of the non-silencing siRNA and La2 siRNA duplexes, respectively. Data are averages of at least three independent experiments. Error bars represent standard deviations.

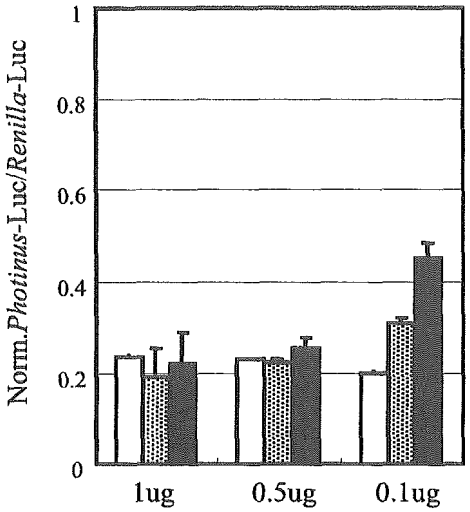

Fig. 7. RNAi induction by short-hairpin RNAs during myogenic differentiation of C2C12 cells. The pRNA-U6.1/Neo/siFluc plasmid (GenScript), which can express a short-hairpin RNA (shRNA) against *Photinus luciferase*, and pRNA-U6.1/Neo empty vector (GenScript) as a control were used. The pGL3-control and phRL-TK plasmids together with a decreasing amount of each of the pRNA-U6.1/Neo/siFluc and pRNA-U6.1/Neo (a negative control) plasmids, from 1 to 0.1 μg, were cotransfected into C2C12 cells. The expression of luciferase was examined 24 h after the transfection. Ratios of normalised target (*Photinus*) luciferase activity to control (*Renilla*) luciferase activity are indicated as in Fig. 2. Open, dotted, and solid bars indicate the data in C2C12 cells that differentiated for 0 (undifferentiated), 2, and 7 days, respectively. Data are averages of at least three independent experiments. Error bars represent standard deviations.

differentiation of C2C12 cell may be caused by losing the stability of functional RISCs in the differentiated C2C12 myotubes.

RNAi induction by short-hairpin RNAs in C2C12 cells

Because Dicer appears to be required for the process of short-hairpin RNAs (shRNAs) into siRNA duplexes, it may be of interest to see if shRNAs can induce RNAi in C2C12 myotubes which barely express *Dicer*. To examine this, we introduced a shRNA expression plasmid against *Photinus* luciferase, pRNA-U6.1/Neo/siRNA, together with the reporter plasmids carrying the *Photinus* and *Renilla* luciferase genes into C2C12 myoblast and myotubes. The results indicate that the shRNA expression plasmid, or shRNAs can induce RNAi in either C2C12 myoblast or myotube (Fig. 7), suggesting that the Dicer protein could be present in those cells. An interesting point to note is that a decrease in the RNAi activity induced by 0.1 μg pRNA-U6.1/Neo/siRNA was observed in C2C12 myotubes that differentiated for 7 days. This may be caused by a possible decrease in the amounts of Dicer and eIF2C1~4 in the cells. To further evaluate the results and a possible relationship between the quantitative level of either Dicer or eIF2C1~4 and RNAi activity, more extensive studies must be conducted.

Integrity of mammalian RNAi

Our previous study has demonstrated that RNAi activity induced by synthetic siRNA duplexes in post mitotic neurons persists for at least 3 weeks, i.e., a long-lasting RNAi activity occurs in mammalian neurons [29]. Our present and previous studies, therefore, suggest that there is a significant difference in the duration of RNAi activity between muscle and neuron, both of which are terminally differentiated and cell cycle-arrested cells. Since neither muscle nor neuron probably undergoes a decrease in the number of functional RISCs by cell division, it may be possible that the stability of functional RISCs could differ between muscle and neuron.

The present observations further suggest the possibility that a little amount of either Dicer or eIF2C1~4 might be sufficient for activation of mammalian RNAi. This seems to be an important point for understanding mammalian RNAi, and further studies on the contribution of either Dicer or eIF2C1~4 to mammalian RNAi must be conducted.

Finally, all the data presented here lead us to the possibility that RNAi may be applicable for a creation of possible model cells and/or model animals for inherited muscular diseases, for example, muscular dystrophy.

Acknowledgments

We thank Drs. Ojima and Takeda (National Institute of Neuroscience) for their technical advice on the preparation of muscle fibers from mouse extensor digitorum longus. This work was supported in part by a Grant-in-Aid from the Japan Society for the Promotion of Science and by research grants from the Ministry of Health, Labor and Welfare in Japan.

References

[1] P.A. Sharp, RNAi and double-strand RNA, Genes Dev. 13 (1999) 139–141.
[2] J.M. Bosher, M. Labouesse, RNA interference: genetic wand and genetic watchdog, Nat. Cell Biol. 2 (2000) E31–E36.
[3] H. Vaucheret, C. Beclin, M. Fagard, Post-transcriptional gene silencing in plants, J. Cell Sci. 114 (2001) 3083–3091.
[4] H. Cerutti, RNA interference: traveling in the cell and gaining functions?, Trends Genet. 19 (2003) 39–46.
[5] S.M. Hammond, E. Bernstein, D. Beach, G.J. Hannon, An RNA-directed nuclease mediates post-transcriptional gene silencing in *Drosophila* cells, Nature 404 (2000) 293–296.
[6] P.D. Zamore, T. Tuschl, P.A. Sharp, D.P. Bartel, RNAi: double-stranded RNA directs the ATP-dependent cleavage of mRNA at 21 to 23 nucleotide intervals, Cell 101 (2000) 25–33.
[7] E. Bernstein, A.A. Caudy, S.M. Hammond, G.J. Hannon, Role for a bidentate ribonuclease in the initiation step of RNA interference, Nature 409 (2001) 363–366.
[8] S.M. Elbashir, W. Lendeckel, T. Tuschl, RNA interference is mediated by 21- and 22-nucleotide RNAs, Genes Dev. 15 (2001) 188–200.

[9] P. Svoboda, P. Stein, H. Hayashi, R.M. Schultz, Selective reduction of dormant maternal mRNAs in mouse oocytes by RNA interference, Development 127 (2000) 4147–4156.
[10] F. Wianny, M. Zernicka-Goetz, Specific interference with gene function by double-stranded RNA in early mouse development, Nat. Cell Biol. 2 (2000) 70–75.
[11] E. Billy, V. Brondani, H. Zhang, U. Muller, W. Filipowicz, Specific interference with gene expression induced by long, double-stranded RNA in mouse embryonal teratocarcinoma cell lines, Proc. Natl. Acad. Sci. USA 98 (2001) 14428–14433.
[12] S. Yang, S. Tutton, E. Pierce, K. Yoon, Specific double-stranded RNA interference in undifferentiated mouse embryonic stem cells, Mol. Cell. Biol. 21 (2001) 7807–7816.
[13] M.R. Player, P.F. Torrence, The 2-5A system: modulation of viral and cellular processes through acceleration of RNA degradation, Pharmacol. Ther. 78 (1998) 55–113.
[14] M. Gale Jr., M.G. Katze, Molecular mechanisms of interferon resistance mediated by viral-directed inhibition of PKR, the interferon-induced protein kinase, Pharmacol. Ther. 78 (1998) 29–46.
[15] S.M. Elbashir, J. Harborth, W. Lendeckel, A. Yalcin, K. Weber, T. Tuschl, Duplexes of 21-nucleotide RNAs mediate RNA interference in cultured mammalian cells, Nature 411 (2001) 494–498.
[16] S. Matsuda, Y. Ichigotani, T. Okuda, T. Irimura, S. Nakatsugawa, M. Hamaguchi, Molecular cloning and characterization of a novel human gene (HERNA) which encodes a putative RNA-helicase, Biochim. Biophys. Acta 1490 (2000) 163–169.
[17] R.H. Nicholson, A.W. Nicholson, Molecular characterization of a mouse cDNA encoding Dicer, a ribonuclease III ortholog involved in RNA interference, Mamm. Genome 13 (2002) 67–73.
[18] P. Provost, D. Dishart, J. Doucet, D. Frendewey, B. Samuelsson, O. Radmark, Ribonuclease activity and RNA binding of recombinant human Dicer, EMBO J. 21 (2002) 5864–5874.
[19] H. Zhang, F.A. Kolb, V. Brondani, E. Billy, W. Filipowicz, Human Dicer preferentially cleaves dsRNAs at their termini without a requirement for ATP, EMBO J. 21 (2002) 5875–5885.
[20] K.S. Yan, S. Yan, A. Farooq, A. Han, L. Zeng, M.M. Zhou, Structure and conserved RNA binding of the PAZ domain, Nature 426 (2003) 468–474.
[21] J. Martinez, A. Patkaniowska, H. Urlaub, R. Luhrmann, T. Tuschl, Single-stranded antisense siRNAs guide target RNA cleavage in RNAi, Cell 110 (2002) 563–574.
[22] N. Doi, S. Zenno, R. Ueda, H. Ohki-Hamazaki, K. Ui-Tei, K. Saigo, Short-interfering-RNA-mediated gene silencing in mammalian cells requires Dicer and eIF2C translation initiation factors, Curr. Biol. 13 (2003) 41–46.
[23] J.D. Rosenblatt, A.I. Lunt, D.J. Parry, T.A. Partridge, Culturing satellite cells from living single muscle fiber explants, In Vitro Cell. Dev. Biol. Anim. 31 (1995) 773–779.
[24] D. Yaffe, O. Saxel, Serial passaging and differentiation of myogenic cells isolated from dystrophic mouse muscle, Nature 270 (1977) 725–727.
[25] H. Hohjoh, RNA interference (RNAi) induction with various types of synthetic oligonucleotide duplexes in cultured human cells, FEBS Lett. 521 (2002) 195–199.
[26] S.M. Hammond, S. Boettcher, A.A. Caudy, R. Kobayashi, G.J. Hannon, Argonaute2, a link between genetic and biochemical analyses of RNAi, Science 293 (2001) 1146–1150.
[27] R.W. Williams, G.M. Rubin, ARGONAUTE1 is required for efficient RNA interference in *Drosophila* embryos, Proc. Natl. Acad. Sci. USA 99 (2002) 6889–6894.
[28] T. Holen, M. Amarzguioui, M.T. Wiiger, E. Babaie, H. Prydz, Positional effects of short interfering RNAs targeting the human coagulation trigger tissue factor, Nucleic Acids Res. 30 (2002) 1757–1766.
[29] K. Omi, K. Tokunaga, H. Hohjoh, Long-lasting RNAi activity in mammalian neurons, FEBS Lett. 558 (2004) 89–95.

Journal of General Virology (2004), 85, 2209–2214 DOI 10.1099/vir.0.79940-0

Short Communication

The adenovirus E1A and E1B19K genes provide a helper function for transfection-based adeno-associated virus vector production

Takashi Matsushita,[1] Takashi Okada,[1] Toshiya Inaba,[2] Hiroaki Mizukami,[1] Keiya Ozawa[1] and Peter Colosi[3]

[1]Division of Genetic Therapeutics, Center for Molecular Medicine, Jichi Medical School, 3311-1 Yakushiji, Minami-kawachi, Kawachi, Tochigi 329-0489, Japan

[2]Department of Molecular Oncology, Research Institute for Radiation Biology and Medicine, Hiroshima University, Hiroshima 734-8553, Japan

[3]Avigen Inc., Alameda, CA, USA

Correspondence
Takashi Okada
tokada@jichi.ac.jp
Peter Colosi
PColosi@avigen.com

Received 26 December 2003
Accepted 17 May 2004

Although the adenoviral E1, E2A, E4 and VA RNA regions are required for efficient adeno-associated virus (AAV) vector production, the role that the individual E1 genes (*E1A*, *E1B19K*, *E1B55K* and *protein IX*) play in AAV vector production has not been clearly determined. E1 mutants were analysed for their ability to mediate AAV vector production in HeLa or KB cells, when cotransfected with plasmids encoding all other packaging functions. Disruption of *E1A* and *E1B19K* genes resulted in vector yield reduction by up to 10- and 100-fold, respectively, relative to the wild-type E1. Interruption of the *E1B55K* and *protein IX* genes had a modest effect on vector production. Interestingly, expression of anti-apoptotic E1B19K cellular homologues such as Bcl-2 or Bcl-x_L fully complemented E1B19K mutants for AAV vector production. These findings may be valuable for the future development of packaging cell lines for AAV vector production.

Adeno-associated virus (AAV)-based vector systems are particularly attractive vehicles for clinical applications requiring long-term *in vivo* gene expression from post-mitotic tissues. AAV vectors have been shown to promote stable expression of a wide variety of transgenes in numerous tissues, including skeletal and cardiac muscle, liver, the central nervous system and retina (Rabinowitz & Samulski, 1998). Overt evidence of inflammation is either minimal or non-existent in target tissues immediately following AAV vector administration. Furthermore, cytotoxic T-lymphocyte responses are not normally elicited to transgene products delivered by AAV vectors, even when such proteins are foreign to the host (Jooss *et al.*, 1998). AAV vectors are considered to be relatively safe because the parental virus is non-pathogenic and unable to replicate in the absence of a co-infecting helper virus. Additionally, current production methods have reduced the regeneration of replication competent wild-type AAV during vector production to undetectable levels (Allen *et al.*, 1997). Finally, the robust protein capsid of AAV makes AAV vectors particularly amenable to existing production methods for protein pharmaceuticals (Gao *et al.*, 2000) and confers upon them desirable drug stability characteristics.

AAV2, the parent virus from which the vector system is derived, is replication defective and requires co-infection of helper viruses to propagate. Adenovirus (Atchinson *et al.*, 1965) and herpes virus (Buller *et al.*, 1981) act as complete helpers and vaccinia virus (Schlehofer *et al.*, 1986) acts as a partial helper. The set of adenoviral (type 2 or 5) genes that facilitate AAV2 propagation has been defined and consists of E1A, E1B55K, the VA RNAs, E2A and E4orf6 (Samulski & Shenk, 1988). E1A acts as a cue to begin virus replication by up-regulating transcription from the *rep* gene promoters, P5 and P19 (Tratschin *et al.*, 1984) and by activating the early adenovirus promoters. E1A is also required to drive the host cell into the S-phase of the cell cycle for viral DNA replication because the AAV encoded proteins are not capable of this function. An adverse effect of E1A is that it stabilizes p53, which leads to apoptosis (Lowe *et al.*, 1993). To prevent this, the E1B55K and the E4orf6 proteins form a complex with p53 and cause it to be degraded through ubiquitin-mediated proteolysis (Querido *et al.*, 1997; Steegenga *et al.*, 1998). Later in infection, E1B55K and E4orf6 form a heterodimer that causes the preferential export of AAV and adenoviral late mRNAs from the nucleus while inhibiting the transit of adenoviral early and cellular mRNAs (Pilder *et al.*, 1986). The 72 kDa DNA-binding protein encoded by E2A has functions in viral DNA replication, viral mRNA processing and export, and AAV promoter regulation (Carter *et al.*, 1992; Ward *et al.*, 1998; Chang & Shenk, 1990). It causes an increase in the intracellular levels of the

single- and double-stranded forms of the AAV genome, the spliced forms of the rep proteins, and dramatically increases capsid protein production. Lastly, the VA RNAs inhibit the interferon-inducible eIF-2 protein kinase, thereby circumventing this cellular anti-viral mechanism from blocking viral protein translation (West *et al.*, 1987).

With respect to E2A, E4orf6 and the VA RNAs, the helper gene requirement for AAV vector and virus production is identical. We and others, have shown that plasmids encoding these genes, when cotransfected into 293 cells along with plasmids encoding rep/cap and a vector, mediate higher levels of vector production than that produced by adenovirus infection (Xiao *et al.*, 1998; Matsushita *et al.*, 1998). This so-called 'triple plasmid' transfection method forms the basis of the current scale-up vector production effort at Avigen and has a respectable mean production efficiency of 1×10^{13} vector genomes produced per 850 cm^2 roller bottle. A report was published describing a method for producing AAV vector in 293 cells using only E4orf6 as the helper gene (Allen *et al.*, 2000). This method requires the use of a heterologous promoter to drive the capsid gene and is about 10-fold less productive than methods using a plasmid encoding all three adenoviral helper genes (unpublished data).

The genes of the E1 region have not been analysed for their contribution to AAV vector production. In this study, we have investigated the role of the *E1A* and *E1B* genes in AAV vector production by using a series of E1 mutant plasmids and cell lines that lack adenoviral genes. E1A was required for efficient vector production. In contrast to the helper requirements for AAV production, our data indicated that *E1B19K* gene greatly augmented vector production, however, *E1B55K* gene did not.

The contributions of each of the component genes from the E1 region to AAV helper function was assessed by creating a set of plasmids with mutations in the *E1A*, *E1B19K*, *E1B55K* or *protein IX* genes and then testing them for their ability to support transfection-based AAV vector production. At least one truncation or one deletion mutation was made for each gene (Fig. 1).

For vector construction the plasmid pE1, which encodes the *E1A*, *E1B19K*, *E1B55K* and *protein IX* genes, was created from Ad2 DNA (Invitrogen). Briefly, the *Afl*III fragment (nt positions 142–5927) of Ad2 was cloned into the *Afl*III site of pBR322 (New England Biolabs) to generate pE1. pE1A-825stop was constructed by the insertion of an adapter (CCGGACTAATTAACTAGT), which includes a stop codon and an *Spe*I site, into the *Bsp*EI site of pE1. Similarly, pE1B19K-1912stop, pE1B55K-2243stop,

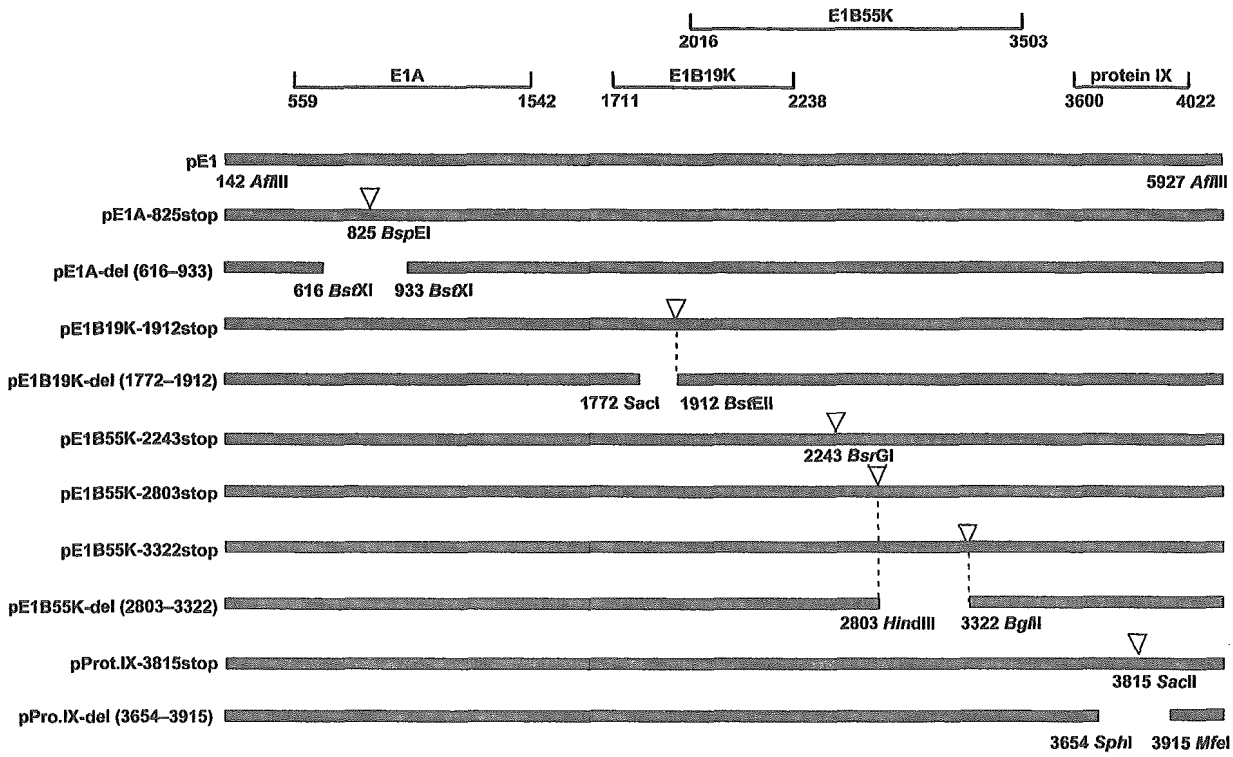

Fig. 1. Schematic representation of plasmids harbouring adenoviral E1 mutants used in this study. A 5·8 kb DNA fragment of adenovirus type 2 was cloned into the *Afl*III site of pBR322. pE1 encodes the entire E1 region, and the E1 mutant plasmids shown here were derived from it. The vertical flags mark the positions of inserted stop codons. The gaps in pE1A, pE1B19K, pE1B55K or pProt.IX constructs represent deletions.

pE1B55K-2803stop and pE1B55K-3322stop were made by the insertion of oligonucleotides into the *Bst*EII, *Bsr*GI, *Hin*dIII and *Bgl*II sites of pE1, respectively. pE1A-del (616–933) has a deletion of a 318 bp segment (positions 616–933 in Ad2). pE1B19K-del (1772–1912) and pE1B55K-del (2803–3322) have the same deletions as *dl337* (Pilder *et al.*, 1984) and *dl338* (Pilder *et al.*, 1986), respectively, used by Samulski & Shenk (1988) to examine E1 helper function for AAV2 production. Briefly, pE1B19K-del (1772–1912) lacks sequences between positions 1772 and 1912, and pE1B55K-del (2803–3322) lacks sequences between positions 2803 and 3322. pProt.IX-3815stop was constructed by the insertion of oligonucleotides into a *Sac*II site. pProt.IX-del (3654–3915) lacks a 262 bp segment (between positions 3654 and 3915 of Ad2).

The helper activities of the various E1 plasmids were assayed by cotransfecting them with a plasmid encoding both an AAV CMV*lacZ* vector and rep/cap (pW4389LacZ), and a plasmid encoding the adenovirus-2 VA RNA, E2A and E4 regions (Pladeno5), into KB or HeLa cells, and then quantifying *lacZ* vector production as described previously (Matsushita *et al.*, 1998). AAV vector was harvested 40 or 72 h after transfection and stocks were prepared by the freeze-thaw method. AAV vector production was quantified by titration of the vector stocks in 293 cells in the presence of adenovirus, followed by X-Gal staining and manual counting by light microscopy. For each experiment, all constructs were tested using triplicate production cultures, and all experiments were conducted at least three times, independently.

Elimination of the entire E1 region resulted in 2 (HeLa cells) to 3 log (KB cells) reduction in vector production relative to production in the presence of pE1, a plasmid encoding the entire E1 region ($P<0{\cdot}01$ by Student's *t*-test) (Fig. 2a, b). Disruption of the *E1A* genes, whether by truncation or deletion, caused 1 (HeLa cells) to 1·5 log (KB cells) reduction in vector production ($P<0{\cdot}01$). Truncations or deletions in the *E1B19K* gene also resulted in substantial reduction in vector production, 1 log in HeLa cells and greater than 2 logs in KB cells ($P<0{\cdot}01$). The lesser severity of the E1B19K mutant in HeLa cells, relative to KB cells, may be due to the relatively high level of Bcl-2 expression in HeLa cells (Liang *et al.*, 1995), or the human papilloma virus E6/E7 genes they harbour. The E6/E7 genes have been shown to facilitate some of the processes in AAV replication (Walz *et al.*, 1997). In most cases, disruption of the *E1B55K* and *protein IX* genes had a modest effect on vector production in either HeLa or KB cells. Two constructs, pE1B55K-2243stop and pProt.IX-3815stop showed fivefold reduction in vector yield in KB cells but little reduction in HeLa cells.

Our results differ substantially from those of Samulski & Shenk (1988) who examined the effect of E1B adenovirus mutants on AAV2 production, DNA replication, and mRNA and protein expression. This group found that an E1B19K adenovirus-2 mutant (*dl337*) mediated efficient AAV production from HeLa cells transfected with a plasmid encoding an AAV wild-type provirus (pSM620) but that

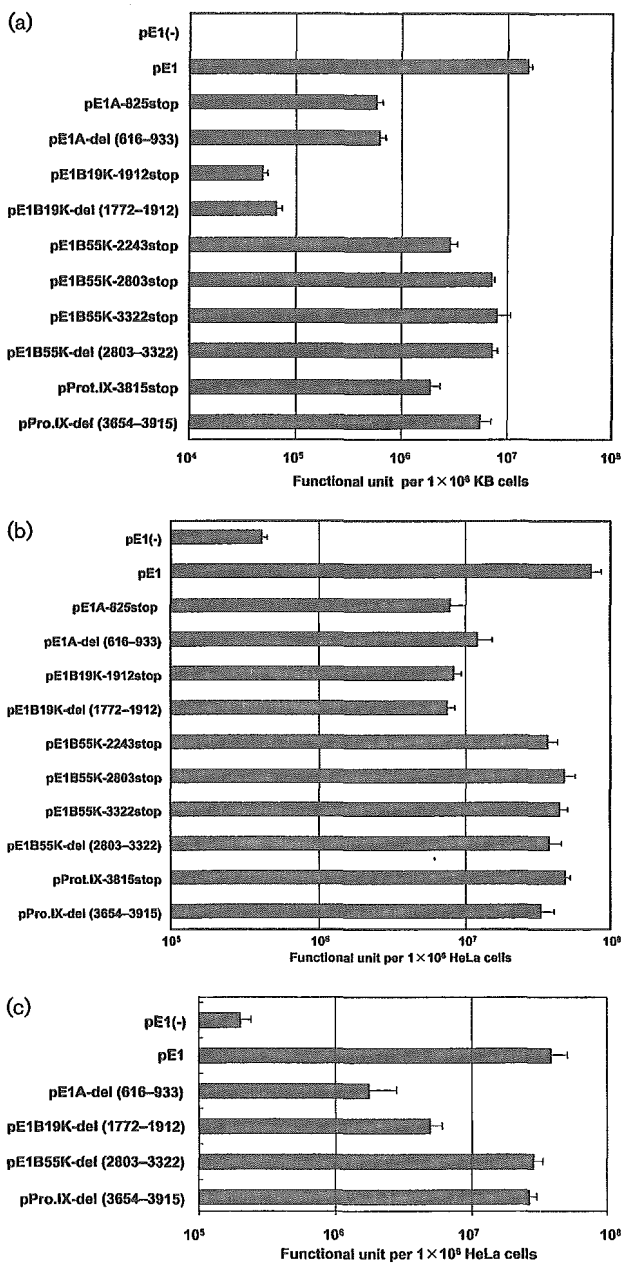

Fig. 2. Comparison of E1 mutant plasmids with respect to AAV helper function in KB (a) and HeLa cells (b) at 72 h after transfection, or in HeLa cells (c) at 40 h after the transfection. AAV *lacZ* vector was produced by the transfection of HeLa or KB cells with pW4389lacZ (encodes rep/cap and an AAV *lacZ* vector) and pladeno 5 (encodes the E2A, E4 and VA RNA regions), in the presence and absence of the indicated E1 plasmids. AAV vector production was assessed by titration of *lacZ* vector in 293 cells. pE1 (-) is identical to pBR322 without the expression cassette. Each bar represents the mean value obtained from triplicate cultures, and the error bar represents the standard deviation.

E1B55K (*dl338*) and E4orf6 (*dl355*) adenovirus mutants did not. AAV virion production was measured at a 40 h time point. The E1B55K and E4orf6 defects were caused by a delay in AAV mRNA accumulation that resulted in delays in viral DNA replication, capsid expression and ultimately virus production. AAV mRNA, DNA and capsid protein concentrations in cultures infected with E1B55K and E4orf6 mutants eventually reached levels seen in cultures infected by wild-type adenovirus but at longer time points, 72–96 h for adenovirus mutants compared with 24–40 h for wild-type adenovirus.

An important difference between our study and that of Samulski & Shenk (1988) was the timing of AAV/AAV vector harvest, 40 h in our study versus 72 h in theirs. Therefore, we examined a subset of the E1 region plasmids in transfection experiments using the same 40 h time point for vector harvest (Fig. 2c). The results were essentially similar to those at the 72 h time point and still differed from those produced by the adenovirus mutants. This observed difference in helper gene requirement may be attributable to technical factors associated with using virus infection or DNA transfection. A possible explanation for the conclusions reached by Samulski & Shenk (1988) might be the differences in the growth rates of the adenovirus mutants tested. The E1B55k mutant, *dl338*, was reported to grow inefficiently (100-fold reduced relative to wild-type) in HeLa cells (Pilder *et al.*, 1986) while the E1B19K mutant, *dl337*, was reported to be less defective (about 10-fold reduced relative to wild-type) (Pilder *et al.*, 1984). The lag in AAV mRNA, DNA and virus production seen with the E1B55K mutant may be simply because of a slow growing helper virus, resulting in low copy numbers of all of the adenovirus helper genes, and may not be directly due to the lack of the mutated gene. The observation that E1B19K is apparently not required for adenovirus mediated AAV production is harder to explain. It is tempting to speculate that the transfection-based production system benefits from additional anti-apoptitic activity provided by E1B19K. If this is true, this requirement does not appear to be cell-type or transfection-reagent specific (calcium phosphate and polycation-based transfection reagents both show an E1B19K effect, data not shown), and may have something to do with the adenoviral helper gene dose or kinetics of expression. Other differences between the two methods of identifying AAV helper function include: transfection method, the packaging of AAV virus versus a vector, and the use of replicating helper (AAV) versus non-replicating plasmid helpers. Full resolution of these issues will require further experimentation.

The adenovirus *E1B19K* gene, and its cellular homologues Bcl-2 and Bcl-x_L, encode anti-apoptotic proteins that function by inhibiting proapoptotic Bcl-2 homologues, such as Bax and Bak, by forming inactive heterodimers with them. To determine whether other anti-apoptotic members of the Bcl-2 family could augment AAV vector production, plasmid vectors expressing the *E1B19K*, *Bcl-2* or *Bcl-x_L* gene

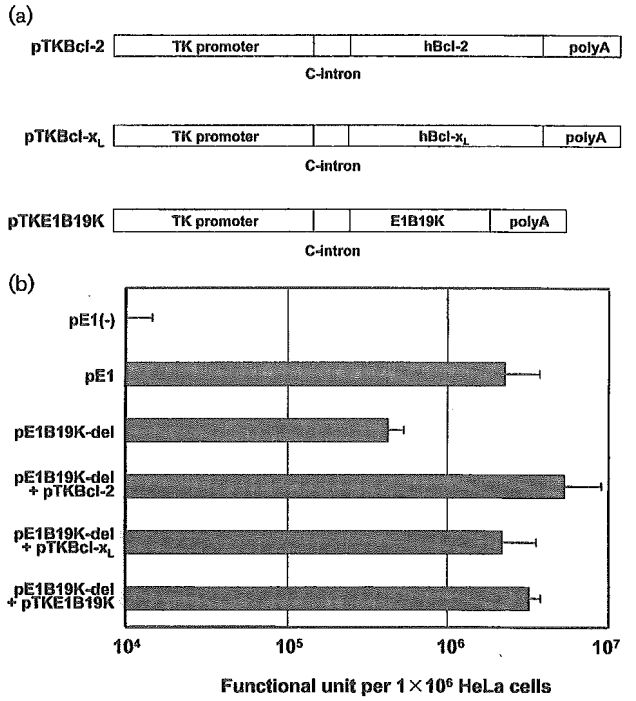

Fig. 3. (a) Schematic representation of Bcl-2, Bcl-x_L and E1B19K expression plasmids. TK promoter, HSV-*tk* promoter; C-intron, chimeric CMV/β-globin intron; polyA, SV40 late polyadenylation signal; hBcl-2, human Bcl-2 cDNA; hBcl-x_L, human Bcl-x_L cDNA; and E1B19K, adenovirus type 2 early region 1B 19 kDa protein gene. (b) Bcl-2 family members complement the vector production defect of an E1B19K mutant in HeLa cells. AAV *lacZ* vector was produced by the transfection of HeLa cells with pW4389lacZ (encodes rep/cap and an AAV *lacZ* vector), pladeno 5 (encodes the E2A, E4 and VA RNA regions), and pE1B19K-del (1772–1912), in the presence and absence of the indicated plasmids expressing Bcl-2 family genes, including E1B19K. AAV vector production was assessed by titration of *lacZ* vector in 293 cells. Each bar represents the mean value of triplicate cultures and the error bar represents the standard deviation.

products were tested for their ability to complement the vector production defect of the E1B19K deletion mutant, pE1B19K-del (1772–1912) (Fig. 3a). pTKPRMCS was assembled by the removal of a *Renilla* luciferase (R*luc*) reporter gene from pRL-TK (Promega) (between the *Nhe*I and *Xba*I sites) and insertion of a multiple cloning site (between the *Kpn*I and *Xba*I sites) from pBluescript II (Stratagene). pTK-Bcl-2 and pTK-Bcl-x_L were created by the insertion of human Bcl-2 and Bcl-x_L cDNA sequences, respectively, into pTKPRMCS. pTK-E1B19K was constructed by the insertion of the E1B19K fragment into pTKPRMCS. As shown in Fig. 3(b), plasmids expressing E1B19K, Bcl-2 or Bcl-x_L restored vector production of the E1B19K deletion mutant to levels equivalent to that produced by the wild-type pE1 plasmid. The use of the medium strength HSV-*tk* promoter to drive the expression

of the Bcl-2 homologues was essential for helper function. CMV-driven constructs produced low vector yields in a dominant fashion and caused a substantial increase in apoptosis (data not shown).

The fact that E1B19K mutants can be complemented by similarly anti-apoptotic cellular homologues such as Bcl-2 or Bcl-x_L suggests a common mechanism, the inhibition of Bak/Bax-mediated apoptosis. Interestingly, no increase in DNA ladder formation is seen in HeLa cells when transfected with E1B19K mutant plasmids relative to wild-type plasmids (data not shown). Consequently, the mechanism of vector production augmentation is not clear.

Current transfection-based AAV vector production methods are sufficient to commercially support gene therapy applications with large doses and small patient populations (e.g. haemophilia, other genetic diseases) or applications with small doses and large patient populations (e.g. Parkinson's disease). Applications with large doses and large patient populations (e.g. heart failure) will be a challenge for transfection-based production methods that scale linearly. Consequently, the construction of a producer cell line that is both helper virus-free, and suspension culture-adaptable, is of great interest. This is a formidable task since many of the viral helper proteins are toxic to the cell either alone (e.g. E2A) or in combination with other helper functions (e.g. E4orf6 and E1B55K, E1A and *rep*). The task is further complicated by genes such as E1B19K that must be expressed in a rather precise manner. Packaging cell lines containing inducible E1 genes, along with the E2a, VA and E4 regions, and an integrated AAV vector have been produced but were found to suffer from relatively low vector yield and substantial production instability (Qiao *et al.*, 2002). Both of these problems were likely due to, or exacerbated by, helper gene toxicity. Our data indicates that one source of toxicity, the inhibition of host mRNA nuclear export mediated by the E4orf6/E1B55K heterodimer, could be eliminated by not including the E1B55K gene in packaging cell lines.

Defining the minimum set of helper genes necessary for efficient vector production is the first step in creating suitable packaging cell lines for AAV vectors. Using our transfection-based assay, we define that set to be E1A, E1B19K, the VA RNAs, E2A and E4orf6 genes.

Acknowledgements

We thank Dr Lawrence H. Boise for providing the Bcl-x_L cDNA, and Dr Michael Lochrie and Dr Matthew Weitzman for manuscript review and helpful comments. We also thank Dr Tatsuya Nomoto and Ms Miyoko Mitsu for their encouragement and support. This work was supported in part by a Grant-in-Aid for Scientific Research on Priority Areas from the Ministry of Education, Science, Sports and Culture of Japan; a grant for Research on Human Genome and Gene Therapy from the Ministry of Health, Labour and Welfare of Japan; Core Research for Evolutional Science and Technology (CREST) of the Japan Science and Technology Corporation (JST); and a Jichi Medical School young investigator award.

References

Allen, J. M., Debelak, D. J., Reynolds, T. C. & Miller, A. D. (1997). Identification and elimination of replication-competent adeno-associated virus (AAV) that can arise by nonhomologous recombination during AAV vector production. *J Virol* **71**, 6816–6822.

Allen, J. M., Halbert, C. L. & Miller, A. D. (2000). Improved adeno-associated virus vector production with transfection of a single helper adenovirus gene, E4orf6. *Mol Ther* **1**, 88–95.

Atchinson, R. W., Casto, B. C. & Hammon, W. M. (1965). Adenovirus-associated defective virus particles. *Science* **149**, 754–756.

Buller, R. M., Janik, J. E., Sebring, E. D. & Rose, J. A. (1981). Herpes simplex virus types 1 and 2 completely help adenovirus-associated virus replication. *J Virol* **40**, 241–247.

Carter, B. J., Antoni, B. A. & Klessig, D. F. (1992). Adenovirus containing a deletion of the early region 2A gene allows growth of adeno-associated virus with decreased efficiency. *Virology* **191**, 473–476.

Chang, L. S. & Shenk, T. (1990). The adenovirus DNA-binding protein stimulates the rate of transcription directed by adenovirus and adeno-associated virus promoters. *J Virol* **64**, 2103–2109.

Gao, G., Qu, G., Burnham, M. S. & 7 other authors (2000). Purification of recombinant adeno-associated virus vectors by column chromatography and its performance *in vivo*. *Hum Gene Ther* **11**, 2079–2091.

Jooss, K., Yang, Y., Fisher, K. J. & Wilson, J. M. (1998). Transduction of dendritic cells by DNA viral vectors directs the immune response to transgene products in muscle fibers. *J Virol* **72**, 4212–4223.

Liang, X. H., Mungal, S., Ayscue, A., Meissner, J. D., Wodnicki, P., Hockenbery, D., Lockett, S. & Herman, B. (1995). Bcl-2 proto-oncogene expression in cervical carcinoma cell lines containing inactive p53. *J Cell Biochem* **57**, 509–521.

Lowe, S. W., Ruley, H. E., Jacks, T. & Housman, D. E. (1993). p53-dependent apoptosis modulates the cytotoxicity of anticancer agents. *Cell* **74**, 957–967.

Matsushita, T., Elliger, S., Elliger, C., Podsakoff, G., Villarreal, L., Kurtzman, G. J., Iwaki, Y. & Colosi, P. (1998). Adeno-associated virus vectors can be efficiently produced without helper virus. *Gene Ther* **5**, 938–945.

Pilder, S., Logan, J. & Shenk, T. (1984). Deletion of the gene encoding the adenovirus 5 early region 1b 21,000-molecular-weight polypeptide leads to degradation of viral and host cell DNA. *J Virol* **52**, 664–671.

Pilder, S., Moore, M., Logan, J. & Shenk, T. (1986). The adenovirus E1B-55K transforming polypeptide modulates transport or cytoplasmic stabilization of viral and host cell mRNAs. *Mol Cell Biol* **6**, 470–476.

Qiao, C., Li, J., Skold, A., Zhang, X. & Xiao, X. (2002). Feasibility of generating adeno-associated virus packaging cell lines containing inducible adenovirus genes. *J Virol* **76**, 1904–1913.

Querido, E., Marcellus, R. C., Lai, A., Charbonneau, R., Teodoro, J. G., Ketner, G. & Branton, P. E. (1997). Regulation of p53 levels by the E1B 55-kilodalton protein and E4orf6 in adenovirus-infected cells. *J Virol* **71**, 3788–3798.

Rabinowitz, J. E. & Samulski, J. (1998). Adeno-associated virus expression systems for gene transfer. *Curr Opin Biotechnol* **9**, 470–475.

Samulski, R. J. & Shenk, T. (1988). Adenovirus E1B 55-Mr polypeptide facilitates timely cytoplasmic accumulation of adeno-associated virus mRNAs. *J Virol* **62**, 206–210.

Schlehofer, J. R., Ehrbar, M. & zur Hausen, H. (1986). Vaccinia virus, herpes simplex virus, and carcinogens induce DNA amplification in a human cell line and support replication of a helpervirus dependent parvovirus. *Virology* **152**, 110–117.

Steegenga, W. T., Riteco, N., Jochemsen, A. G., Fallaux, F. J. & Bos, J. L. (1998). The large E1B protein together with the E4orf6 protein

target p53 for active degradation in adenovirus infected cells. *Oncogene* **16**, 349–357.

Tratschin, J. D., West, M. H., Sandbank, T. & Carter, B. J. (1984). A human parvovirus, adeno-associated virus, as a eucaryotic vector: transient expression and encapsidation of the procaryotic gene for chloramphenicol acetyltransferase. *Mol Cell Biol* **4**, 2072–2081.

Walz, C., Deprez, A., Dupressoir, T., Durst, M., Rabreau, M. & Schlehofer, J. R. (1997). Interaction of human papillomavirus type 16 and adeno-associated virus type 2 co-infecting human cervical epithelium. *J Gen Virol* **78**, 1441–1452.

Ward, P., Dean, F. B., O'Donnell, M. E. & Berns, K. I. (1998). Role of the adenovirus DNA-binding protein in *in vitro* adeno-associated virus DNA replication. *J Virol* **72**, 420–427.

West, M. H., Trempe, J. P., Tratschin, J. D. & Carter, B. J. (1987). Gene expression in adeno-associated virus vectors: the effects of chimeric mRNA structure, helper virus, and adenovirus VA1 RNA. *Virology* **160**, 38–47.

Xiao, X., Li, J. & Samulski, R. J. (1998). Production of high-titer recombinant adeno-associated virus vectors in the absence of helper adenovirus. *J Virol* **72**, 2224–2232.

Gene Therapy (2004) 11, 1370–1377

www.nature.com/gt

RESEARCH ARTICLE

Expansion of genetically corrected neutrophils in chronic granulomatous disease mice by cotransferring a therapeutic gene and a selective amplifier gene

T Hara[1,2], A Kume[1], Y Hanazono[3], H Mizukami[1], T Okada[1], H Tsurumi[2], H Moriwaki[2], Y Ueda[4], M Hasegawa[4] and K Ozawa[1,5]

[1]*Division of Genetic Therapeutics, Center for Molecular Medicine, Jichi Medical School, Tochigi, Japan;* [2]*First Department of Internal Medicine, Gifu University School of Medicine, Gifu, Japan;* [3]*Division of Regenerative Medicine, Center for Molecular Medicine, Jichi Medical School, Tochigi, Japan;* [4]*DNAVEC Research Inc., Ibaraki, Japan; and* [5]*Division of Hematology, Department of Medicine, Jichi Medical School, Tochigi, Japan*

Hematopoietic stem cell gene therapy has not provided clinical success in disorders such as chronic granulomatous disease (CGD), where genetically corrected cells do not show a selective advantage in vivo. To facilitate selective expansion of transduced cells, we have developed a fusion receptor system that confers drug-induced proliferation. Here, a 'selective amplifier gene (SAG)' encodes a chimeric receptor (GcRER) that generates a mitotic signal in response to estrogen. We evaluated the in vivo efficacy of SAG-mediated cell expansion in a mouse disease model of X-linked CGD (X-CGD) that is deficient in the NADPH oxidase gp91^{phox} subunit. Bone marrow cells from X-CGD mice were transduced with a bicistronic retrovirus encoding GcRER and gp91^{phox}, and transplanted to lethally irradiated X-CGD recipients. Estrogen was administered to a cohort of the transplants, and neutrophil superoxide production was monitored. A significant increase in oxidase-positive cells was observed in the estrogen-treated mice, and repeated estrogen administration maintained the elevation of transduced cells for 20 weeks. In addition, oxidase-positive neutrophils were increased in the X-CGD transplants given the first estrogen even at 9 months post-transplantation. These results showed that the SAG system would enhance the therapeutic effects by boosting genetically modified, functionally corrected cells in vivo.
Gene Therapy (2004) **11**, 1370–1377. doi:10.1038/sj.gt.3302317; Published online 1 July 2004

Keywords: *chronic granulomatous disease; selective amplifier gene; respiratory burst; estrogen-binding domain*

Introduction

Gene transfer to hematopoietic stem cells (HSCs) holds promise to provide a long-standing cure of many lymphohematological diseases. One of the candidate disorders is chronic granulomatous disease (CGD), a rare inherited phagocyte dysfunction that renders patients particularly susceptible to catalase-positive microorganisms.[1] The disease is caused by a defect in microbicidal oxidant production, resulting from mutations in the genes encoding four essential subunits of the phagocyte NADPH oxidase (*phox*). The X-linked form of CGD (X-CGD), accounting for about 70% of all cases, is due to genetic mutations in the large subunit of the oxidase cytochrome b_{558}, which is a 91 kDa glycoprotein referred to as gp91^{phox}.[2] A rare autosomal recessive form of CGD results from a defect in the gene encoding p22^{phox}, the small subunit of the cytochrome (about 5%). Other patients have an autosomal recessive trait with a deficiency of either p47^{phox} (20–25%) or p67^{phox} (<5%), which are two soluble proteins in the oxidase complex.

Correspondence: Dr A Kume or Dr K Ozawa, Division of Genetic Therapeutics, Center for Molecular Medicine, Jichi Medical School, 3311-1 Yakushiji, Minamikawachi, Tochigi 329-0498, Japan
Received 7 October 2003; accepted 3 February 2004; published online 1 July 2004

Although prophylactic antibiotics and interferon γ constitute a cornerstone of CGD management and have brought about a better outlook,[3,4] morbidity caused by infection or granulomatous complications remains significant. Allogeneic bone marrow transplantation (BMT) has not been well adopted because of procedure-associated risks and difficulty in finding a suitable donor, but this therapeutic option is increasingly considered for young patients with histocompatible siblings.[5] Recently, a study of patients who underwent nonmyeloablative stem cell transplantation was published, with a better outcome with young patients as well.[6]

Somatic gene therapy targeted at autologous HSCs can bypass problems involved in allotransplantation such as acute graft rejection and graft-versus-host disease.[7] For CGD, correction of only a minority of phagocytes is likely to provide clinical benefit, because a partial chimerism after BMT has freed patients from severe infections and female carriers of X-CGD with as few as 5–10% oxidase-positive neutrophils are often asymptomatic.[8–10] Likewise, preclinical studies with mouse models have provided a rationale for this approach.[11–14] So far, a few phase I clinical gene therapy trials have been conducted, but the percentages of corrected neutrophils have been too low to impact the disease phenotype.[15]

A potential transgene-induced immune reaction remains to be discussed extensively, but maintenance of low-level chimerism in some transplants suggests that rejection by this mechanism is less likely to occur.

Even with the recent refinement of transduction protocols, transducing enough human HSCs is a major challenge to gene therapy for inherited and acquired blood cell disorders.[16] Thus, it is desirable to expand genetically corrected cells in the body, to improve the therapeutic efficacy of stem cell gene therapy. One strategy to achieve this goal is to help their preferential outgrowth through drug selection. On transduction of the target cells with a therapeutic gene and a drug-resistance gene, administering the corresponding cytotoxic drug leads to an increase of genetically modified cells.[17,18] An alternative approach is to confer a direct proliferative advantage on the genetically modified cells, provided that the mitogenic stimulation is restricted to the genetically modified cells in a controllable manner.[19,20]

We have developed a novel system for the selective expansion of transduced cells to compensate for the low frequency of genetically corrected cells.[21–23] The expansion system comprises a fusion protein and a stimulator drug. As a growth signal generator, a chimeric receptor (GcRER) was constructed with the granulocyte colony-stimulating factor (G-CSF) receptor (GcR) and the hormone-binding domain of the estrogen receptor (ER-HBD). The artificial gene encoding the fusion protein was referred to as a 'selective amplifier gene (SAG)'. We showed that transduced hematopoietic stem/progenitor cells were expandable with this system in murine and primate models.[24,25] In the present study, a bicistronic retroviral vector carrying the human gp91^{phox} (hgp91) gene and a modified SAG was evaluated in a mouse model of X-CGD.

Results

Retroviral vector carrying the gp91^{phox} gene and a selective amplifier gene

Figure 1a shows the structure of fusion proteins comprising GcR and ER-HBD. The prototype SAG encodes a fusion protein made up of the full-length mouse GcR and the rat ER-HBD.[21] In ΔGcRER, the G-CSF binding domain (amino acids 5–195 in the full-length GcR) was deleted to free it from the endogenous G-CSF.[21] In addition, the most proximal cytoplasmic tyrosine (position 703) of the mouse GcR was replaced with phenylalanine in ΔY703FGcRER to attenuate the differentiation signal, based on the result that the tyrosine residue was strongly involved in granulocyte maturation.[22]

Figure 1b shows the structure of the retroviral vector used in this study. The vector, MGK/h91GE, was constructed with MFG and MSCV backbones,[26,27] the hgp91 gene and the picornavirus-derived internal ribosome entry site (IRES)-linked ΔY703FGcRER gene.[28] Ecotropic BOSC23 packaging cells were transfected with the MGK/h91GE vector plasmid and the viral supernatant was harvested.[29] Viral titer of the supernatant was estimated to be 5×10^5 particles/ml, by a simplified RNA dot blot protocol along with the plasmid as a reference.[30] Ba/F3 cells and gp91^{phox}-deficient PLB-985 myeloid cells

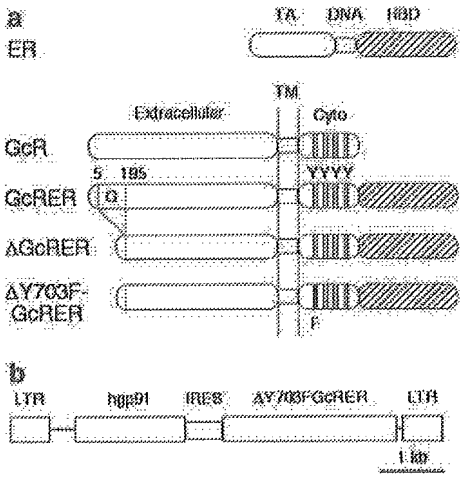

Figure 1 *Structure of selective amplifier gene-encoded proteins and gene transfer vector. (a) GcRER is a fusion protein comprising the full-length mouse G-CSF receptor (GcR) and the hormone-binding domain of the rat estrogen receptor (ER). ΔGcRER is deleted of the G-CSF binding domain of GcR (amino acids 5–195). ΔY703FGcRER has a substitution of phenylalanine for tyrosine 703 in GcR. TA, transactivating domain; DNA, DNA-binding domain; HBD, hormone-binding domain; Extracellular, extracellular domain; TM, transmembrane domain; Cyto, cytoplasmic domain; G, G-CSF binding domain; Y, tyrosine residue; F, phenylalanine substitution for Y703. (b) Schematic representation of bicistronic vector (MGK/h91GE) carrying the human gp91^{phox} gene and a selective amplifier gene. LTR, long-terminal repeat; hgp91, human gp91^{phox} gene; IRES, internal ribosome entry site.*

were transduced with the viral supernatant, and the expression of the vector-encoded hgp91 was confirmed by fluorescence-activated cell sorting (FACS) with 7D5 monoclonal antibody (a gift from Dr M Nakamura, Nagasaki University, Nagasaki, Japan; FACS data not shown).[31,32]

Transduction of X-CGD progenitors

The efficiency of the MGK/h91GE vector was evaluated by transducing X-CGD mouse bone marrow (BM) cells. The X-CGD mouse was created by targeted disruption of the X-linked gp91^{phox} gene, and its phagocytes are devoid of respiratory burst activity.[11] As a result, these mice share many characteristics of the human CGD phenotype, including an elevated susceptibility to *Aspergillus* species. The mice were backcrossed to C57BL/6; subsequently, the X-CGD allele was introduced into the Ly5.1-C57BL/6 congenic background to allow Ly5.1/5.2 chimerism to be analyzed in the BM transplants.

We assessed the *in vitro* responsiveness of vector-transduced cells to estrogen using a clonogenic progenitor assay. BM cells were harvested from male Ly5.1-X-CGD mice treated with intraperitoneal 5-fluorouracil (5-FU) 2 days before. Following prestimulation with stem cell factor (SCF) and interleukin-6 (IL-6) for 2 days, a major part of BM cells was transduced with the MGK/h91GE viral supernatant according to a standard fibronectin-assisted protocol.[33] The remainder part was incubated in the same culture condition as the prestimulation for another 2 days, instead of being transduced with the viral supernatant ('untransduced cells'). Then, untransduced cells and an aliquot of transduced cells were subjected to methylcellulose culture with a cytokine

Table 1 Clonogenic progenitor assay

Growth factors	*Total colony number (% NBT-positive)*	
	Transduced BM	*Untransduced BM*
None	0 (ND)	0 (ND)
IL-3+SCF+G-CSF+Epo	524 (29%)	547 (0%)
E_2	228 (96%)	0 (ND)

Transduced and untransduced X-CGD mouse bone marrow (BM) cells were inoculated onto methylcellulose in duplicate (1×10^5 cells/dish). Colonies were counted at day 10, and an *in situ* NBT test was carried out to detect superoxide production by individual colonies. NBT, nitroblue tetrazolium; ND, not done; IL-3, mouse interleukin-3; SCF, rat stem cell factor; G-CSF, human granulocyte colony-stimulating factor; Epo, human erythropoietin; E_2, estradiol.

combination (SCF, IL-3, erythropoietin (Epo) and G-CSF), 10^{-7} M 17β-estradiol (E_2) alone, or no stimulation. The E_2 concentration that supported optimal growth of the GcRER-transduced murine progenitors was chosen.[21,23] Table 1 summarizes the result of the colony assay at 10 days of growth. No colony was observed in the culture without stimulation, regardless of whether the cells were transduced or untransduced. With the cytokine cocktail, both transduced and untransduced X-CGD BM cells yielded comparable number of colonies (about 500 colonies out of 2×10^5 cells). Most of them were myeloid, and there were a few erythroid and mixed colonies. Thus, transduction with MGK/h91GE did not show positive or negative effect on cytokine-induced colony formation. Finally, the untransduced BM formed no colony in the presence of E_2 alone, as we observed previously.[21,23] In contrast, 10^{-7} M E_2 induced about 200 colonies from 2×10^5 transduced X-CGD BM cells, most of which were granulocyte/monocyte colonies. Considering the very low background colony formation in this assay, these E_2-induced colonies must be derived from vector-transduced progenitors that actually expressed SAG. From the ratio of E_2-induced colonies to cytokine-induced colonies, the *ex vivo* transduction efficiency was estimated to be 44%.

On day 10 of the methylcellulose culture, the colonies were subjected to an *in situ* nitroblue tetrazolium (NBT) test to detect respiratory burst activity. In this assay, most phorbol myristate acetate (PMA)-stimulated wild-type (WT) granulocyte colonies reduced NBT and turned blue (not shown), while the cytokine-induced colonies derived from untransduced X-CGD BM showed no respiratory burst activity (Table 1). As for MGK/h91GE-transduced X-CGD BM, 29% of the cytokine-induced colonies were NBT-positive, while nearly all of the E_2-induced colonies showed a respiratory burst (Table 1 and Figure 2). These results indicated that the SAG/estrogen system selectively expanded genetically modified progenitors *in vitro*, and the estrogen-induced colonies actually coexpressed ΔY703FGcRER and $gp91^{phox}$. NBT positivity in the cytokine-induced colonies (29%) would represent functional transduction efficiency based on $gp91^{phox}$ expression (see Discussion).

In vivo expansion of functionally corrected neutrophils

In parallel with the *in vitro* progenitor assay, the same batch of MGK/h91GE-transduced Ly5.1-X-CGD BM cells

Figure 2 *In situ colony NBT test. X-CGD bone marrow cells were transduced with MGK/h91GE vector and 2×10^5 cells were subjected to methylcellulose culture with 10^{-7} M estradiol. On day 10, the colonies were overlaid with RPMI medium containing NBT and PMA. Nearly all the estrogen-induced colonies were NBT-positive with blue formazan precipitates.*

was transplanted to lethally irradiated male Ly5.2-X-CGD recipients ($n = 8$). Donor-derived Ly5.1 cells rapidly repopulated in the recipients; a series of FACS analysis revealed that the overall white blood cell (WBC) chimerism was 81–91% at 4 weeks post-BMT, and remained above 90% thereafter (FACS data not shown). Following hematopoietic reconstitution, the frequency of oxidase-positive granulocytes in the peripheral blood was monitored by flow cytometry. Leukocytes were loaded with dihydrorhodamine 123 (DHR) and stimulated with PMA.[34] Figure 3 shows representative FACS data of this assay; most PMA-stimulated granulocytes ($Gr1^{high}$) from a WT C57BL/6 mouse produced superoxide to reduce DHR (Figure 3a and e), while granulocytes from an untreated X-CGD mouse did not (Figure 3b and f).

At 6 weeks post-BMT, when the percentage of DHR-positive neutrophils in the transplants was $9.6 \pm 3.2\%$ (range 7.0–17.0%), four out of eight animals were given E_2 intraperitoneally to address whether the drug would induce an expansion of functionally corrected neutrophils. Our preliminary study showed that about 1 mg of E_2 per mouse (ca. 25 g body weight) was required to achieve a serum estrogen level above 10^{-7} M 24 h after injection (unpublished). Based on this observation, the animals were given 1 mg of E_2 in two doses for 3 days, to ensure trough E_2 levels above 10^{-7} M. This treatment was repeated six times with 4-week intervals until 26 weeks post-BMT.

At 2 weeks after the first course of E_2, three out of four challenged mice had increased levels of DHR-positive neutrophils (from 8.3–17.0 to 12.9–67.3%), while one animal had a lowered DHR positivity (from 9.7 to 5.0%). Figure 3c and g shows an E_2-treated mouse that exhibited the most prominent expansion of oxidase-positive neutrophils. In this animal, oxidase-positive granulocytes were increased from 17.0 to 67.3% (Figure 3g). On the other hand, frequencies of DHR-positive granulocytes in the unstimulated mice were unchanged or

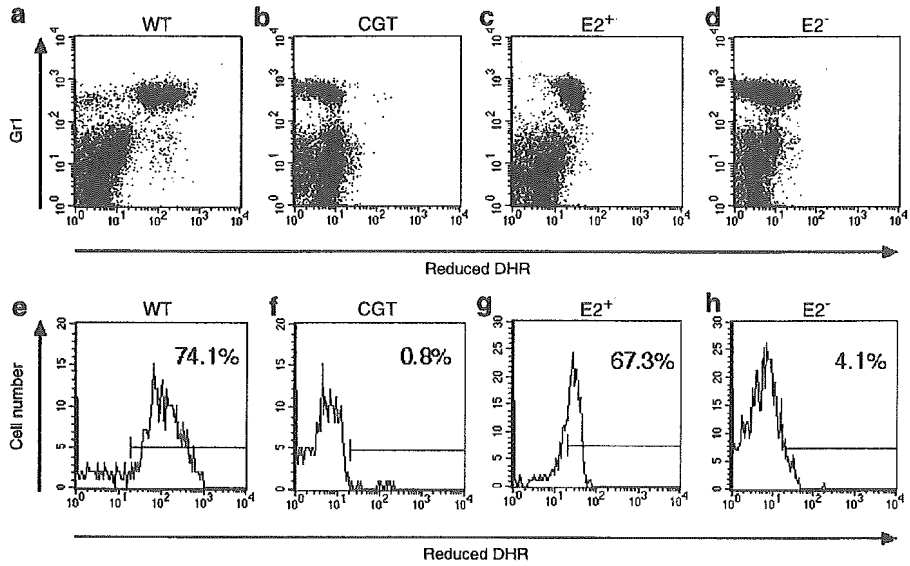

Figure 3 Flow cytometry of DHR assay. Mouse peripheral blood was stimulated with PMA, incubated with DHR and stained with Gr1-PE/Cy5. In the dot plots (a–d), the X-axis represents DHR reduced by superoxide, and the Y-axis represents expression of a granulocyte differentiation marker Gr1. In the histograms (e–h), $Gr1^{high}$-gated cells were shown to highlight superoxide formation by neutrophils. (a and e) A wild-type C57BL/6 mouse (WT). (b and f) An untreated X-CGD mouse (CGD). (c and g) An X-CGD transplant 2 weeks after the first estrogen administration (E_2^+). (d and h) An X-CGD transplant not administered estrogen (E_2^-).

lowered. Only 1.7–10.1% (4.3±3.9%) of neutrophils produced superoxide, and Figure 3d and h shows a FACS analysis of an unstimulated animal. A parallel NBT slide test showed comparable frequencies of oxidase-positive cells in these mice (NBT slides not shown).

Although the initial response to estrogen varied among transplants, repeated E_2 administration led to an increase in respiratory burst-positive neutrophils in these animals. As shown in Figure 4a, the frequency of DHR-positive neutrophils at 16 weeks post-BMT (2 weeks after the third E_2 administration) was elevated in all the treated animals compared to that seen before the drug challenge (from 11.0±4.0 to 35.7±9.1%), and the increase was significant ($P=0.014$ by paired *t*-test). The absolute number of oxidase-positive neutrophils was also significantly increased, as shown in Figure 4b (from 244±211 to 486±302/μl; $P=0.019$ by paired *t*-test).

Prolonged increase in oxidase-positive neutrophils

With repeated E_2 administration, the drug-treated X-CGD transplants maintained a higher level of genetically corrected neutrophils than the untreated animals. A difference between groups was observed 2 weeks after the initial treatment; the drug-treated animals (Group 1) showed higher percentages of DHR-positive neutrophils (27.5±27.8%) than the untreated mice (Group 2; 4.3±3.9%) as shown in Figure 5a ($P=0.043$ by Mann–Whitney *U*-test). This figure also shows that the levels of oxidase-positive granulocytes were significantly higher in Group 1 than Group 2 at most time points during the repeated course of E_2 administration (asterisks in Figure 5a, $P<0.05$ by Mann–Whitney *U*-test). The absolute number of oxidase-positive cells was higher in Group 1 than Group 2 on E_2 treatment as well (asterisks in Figure 5b, $P<0.05$ by Mann–Whitney *U*-test).

At a later time point (38 weeks post-BMT), the treatment was switched. That is, the mice in Group 2

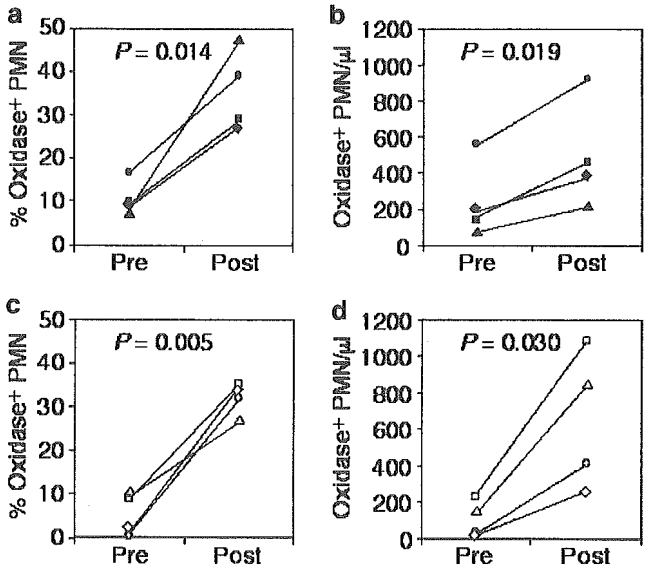

Figure 4 Comparison of oxidase-positive granulocytes before and after estrogen administration. Frequencies (a and c) and absolute numbers (b and d) of oxidase-positive polymorphonuclear leukocytes (PMN) from individual X-CGD transplants are shown. (a and b) Oxidase-positive PMN in Group 1 mice before estrogen administration (Pre; 6 weeks post-BMT) and after the third estrogen injection (Post; 16 weeks post-BMT). The increase was significant by paired t-test (a, $P=0.014$; b, $P=0.019$). (c and d) Oxidase-positive PMN in Group 2 mice before estrogen administration (Pre; 38 weeks post-BMT) and after estrogen injection (Post; 40 weeks post-BMT) at a later time point. The increase was significant by paired t-test (c, $P=0.005$; d, $P=0.030$). Each animal is represented by a different symbol to track the frequency and number of oxidase-positive PMN.

were given E_2 for 3 days, while the animals in Group 1 were left unchallenged. The E_2-stimulated animals showed a remarkable increase in DHR-positive cells. The percentage of DHR-positive granulocytes rose from

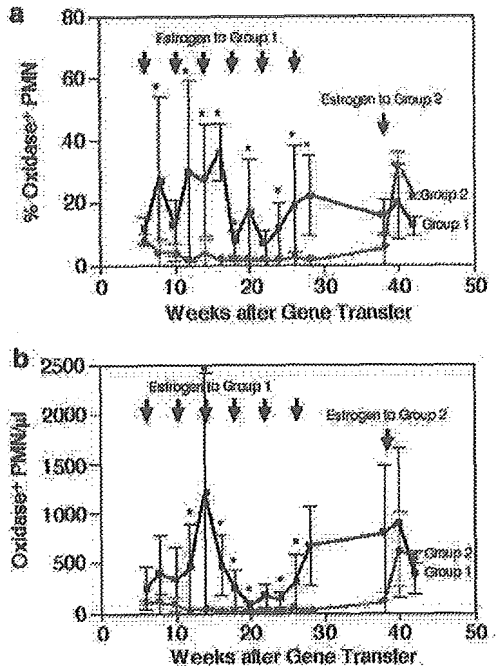

Figure 5 Estrogen-induced expansion of oxidase-positive granulocytes. Graphs indicate the time course of the change in frequency (a) and absolute number (b) of oxidase-positive granulocytes following exposure to estrogen. To mice in Group 1 (n=4), estrogen was given in six courses with 4-week intervals from 6 to 26 weeks post-BMT (black line). Mice in Group 2 (n=4) were given estrogen only once at 38 weeks post-BMT (gray line). Asterisks indicate time points when significantly more oxidase-positive cells existed in Group 1 than Group 2 (P<0.05 by Mann–Whitney U-test).

4.8±4.7 to 31.7±3.8% ($P=0.005$ by paired t-test, Figures 4c and 5a), and the absolute number increased from 96±104 to 638±378/μl ($P=0.030$ by paired t-test, Figures 4d and 5b) in 2 weeks. This result indicated that transduced long-term repopulating cells were maintained in the animals and readily responsive to estrogen, thereby giving rise to an elevated level of corrected neutrophils on drug administration.

During the observation period, the administration of E_2 did not lead to any apparent hematological aberration in the treated mice; none of the recipients of transduced marrow have developed a proliferative disorder, regardless of whether E_2 was administered or not. Apparent feminization was not observed after the periodic estrogen administration in the transplanted male mice.

Discussion

In contrast to successful preclinical gene-transfer studies using mouse models,[13,14] the levels of corrected neutrophils have been too low to impact the CGD phenotype in phase I clinical trials like most gene-transfer attempts targeting human HSCs.[15] In contrast, Fischer and colleagues showed a significant T-lymphocyte reconstitution in a series of patients with X-linked severe combined immunodeficiency (X-SCID) following oncoretrovirus-mediated gene transfer.[35,36] This success largely owes to an extremely strong growth advantage of lymphocyte precursors transduced with a functional common γ chain (γc) gene.[37] However, an excessive growth stimulation may be harmful. Recently, a lymphoproliferative disorder occurred in patients treated in the X-SCID gene therapy following aberrant activation of *LMO2* oncogene by insertional mutagenesis.[38,39] In these patients, a strong and continuous mitogenic stimulation via functional γc may bring about additional events besides *LMO2* activation, finally leading to uncontrolled clonal proliferation. Therefore, for most HSC gene therapy candidate diseases in which a therapeutic gene *per se* does not confer a growth advantage, controlled expansion of transduced stem/progenitor cells is desirable.

For this purpose, we have developed selective amplifier genes,[21] and showed controllable *in vivo* expansion of marker gene-transduced hematopoietic cells in murine and primate models.[24,25] In the present study, we showed that functionally corrected cells were expandable using the SAG system in an actual disease model of CGD. An *in vitro* NBT assay showed that estrogen specifically induced functionally corrected colonies. It is currently unclear why gene transfer efficiency based on the total number of colonies (44%) differed from that based on NBT positivity (29%). At present, we consider the latter estimation (29% based on NBT positivity) as more accurate and reliable, because the former is based on an indirect calculation with colony number, which inherently includes fluctuation.

We also showed an *in vivo* expansion of corrected neutrophils. Following estrogen stimulation, the ratio and number of oxidase-positive granulocytes were elevated, and repeated drug administration maintained an increased level of corrected cells. Furthermore, superoxide-producing cells increased remarkably in the transplants given estrogen at a later time point (Group 2 in Figure 5), suggesting that transduced long-term repopulating cells remain responsive to estrogen and that on-demand expansion of functional neutrophils is feasible in CGD. As mentioned, we observed that the initial response to estrogen varied among transplants in Group 1, and the reason for this variation is yet to be clarified. Considering that the mice in Group 2 responded to E_2 with little deviation at a later time point, the early E_2 administration to Group 1 may account, in part, for this variation. The mice in Group 1 were given E_2 at 6 weeks post-BMT, when the donor-derived hematopoiesis might not have reached a steady state and varied among animals considerably.

Including the present study, we have not encountered a neoplastic outgrowth of SAG-transduced cells in the animals examined thus far, including a primate system.[24,25] Blau and colleagues have presented another conditional expansion system in which an FK506-binding protein 12-based fusion receptor is activated by a dimerizing crosslinker, and no cancerous event has been reported.[19,40,41] Still more extensive studies are required to clear safety issues concerning uncontrolled proliferation. We are carrying out serial transplantation of SAG-transduced BM in an attempt to predict whether such complications would arise in a longer-term follow-up. In addition, large animal studies with clinically relevant protocols are mandatory to address the safety and feasibility of regulated cell expansion in HSC gene therapy.

Materials and methods

Plasmid construction

To transduce X-CGD hematopoietic cells with the hgp91 gene and a modified SAG, a bicistronic retrovirus vector was constructed. The vector, MGK/h91GE, had a hybrid backbone (MGK) comprising the long-terminal repeats (LTRs) and the primer-binding site from MSCV and the *gag* through to the *env* initiation codon from MFG.[26,27,42] The 5′-half of hgp91 cDNA (from the initiation codon to the internal *AseI* site) was derived from pBS/hgp91,[31] by amplification with the polymerase chain reaction (PCR) (upstream primer, 5′-TCTGCCACCATGGGGAACT-3′, and downstream primer, 5′-GCAAGGCCAATGAA GAAGAT-3′) to create an *NcoI* site at the initiation codon. The 3′-half of hgp91 (from the internal *AseI* site to the stop codon) was PCR-amplified on pBS/hgp91 using an upstream primer, 5′-GGCATCACTGGAGTTGTCA-3′, and a downstream primer, 5′-GAGGATCCTTA GAAGTTTTCCTTGTTGAA-3′, to add a *Bam*HI site at the 3′ end. The fragments were cloned into the *NcoI–BamHI* site of MGK by trimolecular ligation to yield MGK/hgp91.[42] The 5′ half of the SAG (from the initiation codon to the internal *DraIII* site) was PCR-amplified on pBS/ΔY703FGcRER,[22] with 5′-AAATGGGACCTCTGG GAGCCTGCACCCTG-3′ as an upstream primer and a *DraIII* site-linked downstream primer (5′-AGAA CAGCTGCACACTCACT-3′) to create a *Ppu*MI site at the initiation codon. The 3′ half of the SAG (from the *DraIII* site to the stop codon) was PCR-amplified on pBS/ ΔY703FGcRER with 5′-AAGGCCCCCACCATCAGA CT-3′ as an upstream primer and an *XhoI* site-linked downstream primer (5′-CTGGCTCGAGTCAGATGG TGTTGGGGAAG-3′) to add an *XhoI* site to the 3′ end. The fragments were cloned into the *Ppu*MI–*XhoI* site of pCGI,[43] which contains the encephalomyocarditis virus-derived IRES,[28] by trimolecular ligation. Subsequently, the IRES-ΔY703FGcRER cassette was obtained as a *Bam*HI–*XhoI* fragment, and inserted between the hgp91 and the 3′-LTR of MGK/hgp91, resulting in the final construct MGK/h91GE (Figure 1b).

Animals

Targeted disruption of the X-linked gp91^{phox} gene in the mouse was described.[11] The X-CGD mice backcrossed to Ly5.2-C57BL/6 were a gift from Dr MC Dinauer (Indiana University, Indianapolis, IN, USA). The X-CGD mice were crossed with Ly5.1-congenic C57BL/6 mice, and both Ly5.1- and Ly5.2-X-CGD mice were maintained under specific pathogen-free conditions. The animals were given free access to autoclaved food and ultraviolet-irradiated water and treated according to the institutional codes governing animal rights. WT Ly5.2-C57BL/6 mice were purchased from Clea Japan (Tokyo, Japan).

Retroviral transduction

Ecotropic retroviral supernatant was prepared by transient transfection of BOSC23 packaging cells (American Type Culture Collection CRL-11554, Manassas, VA, USA) with MGK/h91GE using Lipofectamine (Invitrogen, Grand Island, NY, USA), following the manufacturer's protocol.[29] X-CGD mouse BM cells were retrovirally transduced using a fibronectin-assisted protocol.[25,33] Male Ly 5.1-X-CGD mice were injected intraperitoneally with 150 mg/kg 5-FU (Kyowa Hakko, Tokyo, Japan), and BM cells were collected 2 days postinjection. Low-density mononuclear cells were separated using Lympholyte-M (Cedarlane Laboratories, Hornby, Canada) and stimulated for 2 days with α-Minimum Essential Medium (Invitrogen) containing 100 ng/ml recombinant rat SCF (provided by Amgen, Thousand Oaks, CA, USA) and 100 U/ml recombinant human IL-6 (provided by Ajinomoto, Kawasaki, Japan).[44] The cells were then incubated in the fresh viral supernatant on plates precoated with recombinant human fibronectin fragment CH-296 (RetroNectin; provided by Takara Bio, Otsu, Japan) for 2 days under the same conditions. Supernatant infection was repeated five times during transduction, and the manipulated cells were recovered using Cell Dissociation Buffer (Invitrogen). As a negative control, an aliquot of the prestimulated cells was incubated in α-Minimum Essential Medium containing SCF and IL-6 for another 2 days ('untransduced cells').

Clonogenic progenitor assay

Hematopoietic progenitors were assayed using StemPro Methylcellulose Medium (Invitrogen) supplemented with appropriate growth factors. Transduced and untransduced X-CGD mouse BM cells were seeded onto Petri dishes at a density of 1×10^5 cells/dish in 1 ml of StemPro medium containing either no growth factor, 10^{-7} M E_2 (Sigma, St Louis, MO, USA) alone, or a cytokine cocktail of 2 U/ml recombinant human Epo (provided by Chugai Pharmaceuticals, Tokyo, Japan), 100 ng/ml SCF, 20 ng/ml recombinant human G-CSF (provided by Chugai Pharmaceuticals) and 100 U/ml IL-3.[21–23] After 10 days of incubation, colonies were counted and assayed for respiratory burst activity using an *in situ* NBT test (NBT from Sigma).[45] A one-fifth volume of NBT-saturated RPMI-1640 medium (Invitrogen) containing 100 ng/ml PMA (Sigma) and 5% human serum albumin (Baxter Healthcare, Deerfield, IL, USA) was layered onto the methylcellulose culture and incubated at 37°C. After 1 h of incubation, the dishes were examined on an inverted microscope, and the colonies with blue formazan precipitates were scored as NBT-positive.

BMT and estrogen administration

For hematopoietic reconstitution with retrovirally transduced Ly5.1-X-CGD BM cells, 8–10-week-old male Ly5.2-X-CGD recipients were lethally irradiated (split dose of 11 Gy at an interval of 3 h with ^{137}Cs using Gammacell 40, Nordion International, Kanata, Canada) and transplanted with the transduced BM cells. A total of $2–3 \times 10^6$ cells per recipient were given by tail vein injection. WBCs were stained with a fluorescein isothiocyanate-conjugated anti-Ly5.2 antibody (Pharmingen, San Diego, CA) and a phycoerythrin (PE)-conjugated anti-Ly5.1 antibody (Pharmingen) to measure chimerism with a FACScan (Becton Dickinson, San Jose, CA, USA). After hematopoietic reconstitution, one half of the transplanted mice were administered with estrogen (Group 1). Starting from 6 weeks post-BMT, the mice were intraperitoneally given 0.5 mg of E_2 dipropionate (Ovahormon Depot from Teikoku Hormone MFG, Tokyo, Japan) twice for 3 days. The E_2 administration was repeated every 4 weeks until 28 weeks after BMT. At 40 weeks, E_2 administration was switched so that the formerly unstimulated mice were challenged with E_2 (Group 2).

Peripheral blood counts and measurement of respiratory burst activity

A complete blood cell count (CBC) was performed using tail vein blood on a PC-608 particle counter (Erma, Tokyo, Japan) according to the manufacturer's recommendations. Blood smears were stained with Wright–Giemsa using standard methods and examined at × 500 for differential analysis.

Superoxide production by peripheral leukocytes was assayed using the NBT slide test of Buescher with slight modification.[10] Fresh whole blood from the tail vein was placed on a glass slide and incubated at 37°C in a humidified chamber until it had clotted. The clot was gently removed, and the slide was rinsed in phosphate-buffered saline (PBS) to free it of erythrocytes, then covered with NBT-saturated RPMI-1640 medium containing 100 ng/ml PMA and 5% human serum albumin. After incubation at 37°C for 20 min, the slide was rinsed in PBS, fixed in absolute methanol for 60 s, and counterstained with 1% safranine-O (Sigma) to identify nuclear morphology. Superoxide production by peripheral leukocytes was assayed using flow cytometry by loading the cells with DHR (Sigma) as described.[13,14,34] Mouse whole blood was incubated with 30 μM DHR at 37°C for 5 min and stimulated with 5 μg/ml PMA at 37°C for 30 min. After erythrocytes were lysed with Lysis buffer (150 mM NH_4Cl, 20 mM $NaHCO_3$, 1 mM EDTA), the cells were stained with a biotinylated anti-Gr1 antibody (Pharmingen) plus PE/Cy5-conjugated streptavidin (DAKO, Glostrup, Denmark) and analyzed with a FACScan. Data were statistically analyzed using the Mann–Whitney *U*-test and the paired *t*-test with StatView software (SAS Institute, Cary, NC, USA).

Acknowledgements

We thank Dr MC Dinauer for X-CGD mice, and Dr M Nakamura for 7D5 monoclonal antibody. We are also grateful to Amgen for SCF, Ajinomoto for IL-6, Chugai Pharmaceuticals for Epo and G-CSF, and Takara Bio for RetroNectin. This work was supported in part by grants from the Ministry of Education, Culture, Sports, Science and Technology of Japan, and the Ministry of Health, Labor and Welfare of Japan.

References

1 Curnutte JT, Dinauer MC. Genetic disorders of phagocyte killing. In: Stamatoyannopoulos G, Majerus PW, Perlmutter RM, Varmus H (eds). *The Molecular Basis of Blood Diseases*. W.B. Saunders: Philadelphia, 2001, pp 539–563.
2 Winkelstein JA *et al*. Chronic granulomatous disease: report on a national registry of 368 patients. *Medicine* 2000; **79**: 155–169.
3 Weening RS, Kabel P, Pijman P, Roos D. Continuous therapy with sulfamethoxazole-trimethoprim in patients with chronic granulomatous disease. *J Pediatr* 1983; **103**: 127–130.
4 The International Chronic Granulomatous Disease Cooperative Study Group. A controlled trial of interferon gamma to prevent infection in chronic granulomatous disease. *N Engl J Med* 1991; **324**: 509–516.
5 Seger RA *et al*. Treatment of chronic granulomatous disease with myeloablative conditioning and an unmodified hemopoietic allograft: a survey of the European experience, 1985–2000. *Blood* 2002; **100**: 4344–4350.
6 Horwitz ME *et al*. Treatment of chronic granulomatous disease with nonmyeloablative conditioning and a T-cell-depleted hematopoietic allograft. *N Engl J Med* 2001; **344**: 881–888.
7 Kume A, Dinauer MC. Gene therapy for chronic granulomatous disease. *J Lab Clin Med* 2000; **135**: 122–128.
8 Kamani N *et al*. Marrow transplantation in chronic granulomatous disease: an update, with 6-year follow-up. *J Pediatr* 1988; **113**: 697–700.
9 Woodman RC *et al*. A new X-linked variant of chronic granulomatous disease characterized by the existence of a normal clone of respiratory burst-competent phagocytic cells. *Blood* 1995; **85**: 231–241.
10 Buescher ES, Alling DW, Gallin JI. Use of an X-linked human neutrophil marker to estimate timing of lyonization and size of the dividing stem cell pool. *J Clin Invest* 1985; **76**: 1581–1584.
11 Pollock JD *et al*. Mouse model of X-linked chronic granulomatous disease, an inherited defect in phagocyte superoxide production. *Nat Genet* 1995; **9**: 202–209.
12 Jackson SH, Gallin JI, Holland SM. The $p47^{phox}$ mouse knock-out model of chronic granulomatous disease. *J Exp Med* 1995; **182**: 751–758.
13 Björgvinsdóttir H *et al*. Retroviral-mediated gene transfer of $gp91^{phox}$ into bone marrow cells rescues defect in host defense against *Aspergillus fumigatus* in murine X-linked chronic granulomatous disease. *Blood* 1997; **89**: 41–48.
14 Mardiney III M *et al*. Enhanced host defense after gene transfer in the murine $p47^{phox}$-deficient model of chronic granulomatous disease. *Blood* 1997; **89**: 2268–2275.
15 Malech HL *et al*. Prolonged production of NADPH oxidase-corrected granulocytes after gene therapy of chronic granulomatous disease. *Proc Natl Acad Sci USA* 1997; **94**: 12133–12138.
16 Emery DW *et al*. Hematopoietic stem cell gene therapy. *Int J Hematol* 2002; **75**: 228–236.
17 Moscow JA *et al*. Engraftment of *MDR1* and NeoR gene-transduced hematopoietic cells after breast cancer chemotherapy. *Blood* 1999; **94**: 52–61.
18 Abonour R *et al*. Efficient retrovirus-mediated transfer of the multidrug resistance 1 gene into autologous human long-term repopulating hematopoietic stem cells. *Nat Med* 2000; **6**: 652–658.
19 Neff T, Blau CA. Pharmacologically regulated cell therapy. *Blood* 2001; **97**: 2535–2540.
20 Kume A *et al*. Selective expansion of transduced cells for hematopoietic stem cell gene therapy. *Int J Hematol* 2002; **76**: 299–304.
21 Ito K *et al*. Development of a novel selective amplifier gene for controllable expansion of transduced hematopoietic cells. *Blood* 1997; **90**: 3884–3892.
22 Matsuda KM *et al*. Development of a modified selective amplifier gene for hematopoietic stem cell gene therapy. *Gene Therapy* 1999; **6**: 1038–1044.
23 Xu R *et al*. A selective amplifier gene for tamoxifen-inducible expansion of hematopoietic cells. *J Gene Med* 1999; **1**: 236–244.
24 Hanazono Y *et al*. *In vivo* selective expansion of gene-modified hematopoietic cells in a nonhuman primate model. *Gene Therapy* 2002; **9**: 1055–1064.
25 Kume A *et al*. *In vivo* expansion of transduced murine hematopoietic cells with a selective amplifier gene. *J Gene Med* 2003; **5**: 175–181.
26 Hawley RG, Lieu FHL, Fong AZC, Hawley TS. Versatile retroviral vectors for potential use in gene therapy. *Gene Therapy* 1994; **1**: 136–138.
27 Dranoff G *et al*. Vaccination with irradiated tumor cells engineered to secrete murine granulocyte-macrophage colony-stimulating factor stimulates potent, specific, and long-lasting anti-tumor immunity. *Proc Natl Acad Sci USA* 1993; **90**: 3539–3543.

28 Duke GM, Hoffman MA, Palmenberg AC. Sequence and structural elements that contribute to efficient encephalomyocarditis virus RNA translation. *J Virol* 1992; **66**: 1602–1609.
29 Pear WS, Nolan GP, Scott ML, Baltimore D. Production of high-titer helper-free retroviruses by transient transfection. *Proc Natl Acad Sci USA* 1993; **90**: 8392–8396.
30 Onodera M *et al*. A simple and reliable method for screening retroviral producer clones without selectable markers. *Hum Gene Ther* 1997; **8**: 1189–1194.
31 Zhen L *et al*. Gene targeting of X chromosome-linked chronic granulomatous disease locus in a human myeloid leukemia cell line and rescue by expression of recombinant gp91^{phox}. *Proc Natl Acad Sci USA* 1993; **90**: 9832–9836.
32 Nakamura M *et al*. Monoclonal antibody 7D5 raised to cytochrome b_{558} of human neutrophils: immunocytochemical detection of the antigen in peripheral phagocytes of normal subjects, patients with chronic granulomatous disease, and their carrier mothers. *Blood* 1987; **69**: 1404–1408.
33 Hanenberg H *et al*. Colocalization of retrovirus and target cells on specific fibronectin fragments increases genetic transduction of mammalian cells. *Nat Med* 1996; **2**: 876–882.
34 Vowells SJ *et al*. Flow cytometric analysis of the granulocyte respiratory burst: a comparison study of fluorescent probes. *J Immunol Methods* 1995; **178**: 89–97.
35 Cavazzana-Calvo M *et al*. Gene therapy of human severe combined immunodeficiency (SCID)-X1 disease. *Science* 2000; **288**: 669–672.
36 Hacein-Bey-Abina S *et al*. Sustained correction of X-linked severe combined immunodeficiency by *ex vivo* gene therapy. *N Engl J Med* 2002; **346**: 1185–1193.
37 Kume A *et al*. Selective growth advantage of wild-type lymphocytes in X-linked SCID recipients. *Bone Marrow Transplant* 2002; **30**: 113–118.
38 Hacein-Bey-Abina S *et al*. A serious adverse event after successful gene therapy for X-linked severe combined immunodeficiency. *N Engl J Med* 2003; **348**: 255–256.
39 Kohn DB, Sadelain M, Glorioso JC. Occurrence of leukaemia following gene therapy of X-linked SCID. *Nat Rev Cancer* 2003; **3**: 477–488.
40 Jin L *et al*. *In vivo* selection using a cell-growth switch. *Nat Genet* 2000; **26**: 64–66.
41 Neff T *et al*. Pharmacologically regulated *in vivo* selection in a large animal. *Blood* 2002; **100**: 2026–2031.
42 Kume A *et al*. Lymphoid reconstitution in X-linked severe combined immunodeficient mice by retrovirus-mediated gene transfer. *Proc Jpn Acad* 2002; **78**: 211–216.
43 Kume A *et al*. Long-term tracking of murine hematopoietic cells transduced with a bicistronic retrovirus containing CD24 and EGFP genes. *Gene Therapy* 2000; **7**: 1193–1199.
44 Yasueda H *et al*. High-level direct expression of semi-synthetic human interleukin-6 in *Escherichia coli* and production of N-terminus Met-free product. *Bio/Technology* 1990; **8**: 1036–1040.
45 Sekhsaria S *et al*. Peripheral blood progenitors as a target for genetic correction of p47^{phox}-deficient chronic granulomatous disease. *Proc Natl Acad Sci USA* 1993; **90**: 7446–7450.

Original Paper

Pharmacology

Pharmacology 2004;72:26–32
DOI: 10.1159/000078629

Received: July 25, 2003
Accepted after revision: January 30, 2004

Effects of Pranidipine, a Novel Calcium Channel Antagonist, on the Progression of Left Ventricular Dysfunction and Remodeling in Rats with Heart Failure

Mir Imam Ibne Wahed[a] Kenichi Watanabe[a] Meilei Ma[a] Mikio Nakazawa[b] Toshihiro Takahashi[c] Go Hasegawa[d] Makoto Naito[d] Tadashi Yamamoto[e] Makoto Kodama[f] Yushifusa Aizawa[f]

[a]Department of Clinical Pharmacology, Faculty of Pharmaceutical Sciences, Niigata University of Pharmacy and Applied Life Sciences; [b]Department of Medical Technology, School of Health Sciences; [c]Radioisotope Center; [d]Second Department of Pathology; [e]Department of Structural Pathology, Institute of Nephrology, and [f]First Department of Medicine, Niigata University School of Medicine, Niigata, Japan

Key Words
Calcium channel antagonists · Pranidipine · Heart failure · Remodeling · TGF-β_1 · Fibrosis

Abstract
The cardioprotective properties of pranidipine were studied in a rat model of heart failure after autoimmune myocarditis. Twenty-eight days after immunization the surviving rats were divided into three groups and received oral treatment of 0.03 mg/kg/day (group 0.03) or 0.3 mg/kg/day (group 0.3) of pranidipine or vehicle (group V) for 1 month. High-dose pranidipine (group 0.3) improved the survival rate, and significantly reduced heart weight, heart weight to body weight ratio, myocardial fibrosis, central venous pressure and left ventricular end-diastolic pressure than low-dose pranidipine (group 0.03) and group V. Pranidipine at high dose also decreased the left ventricular systolic and diastolic dimensions, and increased fractional shortening compared with group V. The increase in level of TGF-β_1 and collagen-III mRNA were suppressed by pranidipine in a dose-dependent manner. Our results indicated that pranidipine has cardioprotective effects on heart failure, and that the beneficial effect can be partly explained by attenuation of fibrotic response through suppression of TGF-β_1 and collagen-III mRNA expression, and regression of myocyte hypertrophy.

Introduction

Dilated cardiomyopathy is a set of heterogeneous diseases of left ventricular dysfunction due to unknown etiology. There are a variety of clinical courses and pathologic findings [1, 2]. One of the possible causes of dilated cardiomyopathy is considered to be a sequel to myocarditis [3]. Two mechanisms by which myocarditis develop into dilated cardiomyopathy have been proposed: one is persistent viral infection and the other is progressive autoimmune myocardial injury [4, 5]. Human myocarditis can be classified into lymphocytic myocarditis and giant cell myocarditis according to the histopathological findings. Giant cell myocarditis is a fatal disease and survivors are more likely to develop dilated cardiomyopathy than pa-

KARGER
Fax + 41 61 306 12 34
E-Mail karger@karger.ch
www.karger.com

0031–7012/04/0721–0026$21.00/0
Accessible online at:
www.karger.com/pha

Prof. Kenichi Watanabe
Department of Clinical Pharmacology, Faculty of Pharmaceutical Sciences
Niigata University of Pharmacy and Applied Life Sciences
5-13-2 Kamishin-ei-cho, Niigata 950-2081 (Japan)
Tel. +81 25 2693170, Fax +81 25 2681230, E-Mail watanabe@niigata-pharm.ac.jp

tients with lymphocytic myocarditis [4–6]. Our rat model of autoimmune myocarditis is characterized by extensive myocardial necrosis, congestive heart failure and the appearance of multinucleated giant cells and reflective to human giant cell myocarditis [7–9].

The therapeutic efficacy of calcium channel antagonists in the treatment of patients with hypertension, supraventricular arrhythmia and ischemic heart diseases is well known. Primarily, calcium channel antagonist acts at the voltage-gated L-type calcium channels where they inhibit calcium influx into arterial smooth muscle cells to decrease vascular contractility and arterial tone [10, 11]. In addition, calcium channel antagonists have a cytoprotective effect independent of their calcium channel blocking action [12, 13]. Calcium antagonist also possesses lipid antioxidant properties which may contribute to their role in atherosclerosis [14]. However, several studies indicated that calcium channel antagonists may worsen heart failure and increase the risks of death in patients with advanced left ventricular dysfunction [15–17].

Pranidipine is a new long-acting dihydropyridine calcium antagonist and has been demonstrated to have the most potent and longest-lasting antihypertensive actions in normotensive and various hypertensive animal models [18, 19]. Pranidipine has a direct venodilator effect, and exerts a greater reduction in mean circulatory filling pressure – an index of body venous tone than either nifedipine or amlodipine [20]. The stronger venodilatory action of pranidipine may be explained by the unique mechanism that enhances NO-induced cGMP-independent relaxation [21, 22]. Pranidipine has been shown to prevent myocardial remodeling accompanied by cardiac dysfunction and abnormal cardiac gene expressions after myocardial infarction in rats [23]. It has protected progressive left ventricular dilatation and wall thinning in an avian model of dilated cardiomyopathy [24]. Pranidipine was shown to protect kidneys and brain of salt-sensitive Dahl rats from pathological changes and found to reduce collagen levels [25]. We investigated the effects of long-term treatment with pranidipine on the progression of myocardial dysfunction and remodeling in rats with heart failure after experimental autoimmune myocarditis [7–9].

Methods

Animals and Medication

Nine-week-old male Lewis rats purchased from Charles River Japan Inc. (Kanagawa, Japan) were immunized with pig myosin according to a modification of the procedure described previously [7–9]. The morbidity of experimental autoimmune myocarditis was 100% in rats immunized by this procedure [7–9]. Twelve (25%) of 48 rats died between days 14 and 28 after immunization. Twenty-eight days after immunization, the surviving rats were divided into three groups for the oral administration of either 0.03 mg/kg/day (group 0.03, n = 11) or 0.3 mg/kg/day (group 0.3, n = 10) of pranidipine, or vehicle (0.5% methylcellulose, group V, n = 15) for 1 month. Age-matched Lewis rats that received no treatment were used as normal control (group N, n = 10). The animals used in this study were cared for in accordance with our institute's guidelines on animal experimentation [9].

Measurement of Blood Pressure and Heart Rate in Rats with Heart Failure

The blood pressure and heart rate of conscious rats were measured on day 0, before treatment and on days 14 and 28 of oral administration of pranidipine or vehicle. After 4 h of oral treatment, when the drug exhibited the maximal hypotensive effect, heart rate, systolic blood pressure (SBP) and mean blood pressure (MBP) were measured by the tail-cuff plethysmographic method (Softron BP-98A, Tokyo, Japan).

Hemodynamic Study

After drug administration for 1 month, hemodynamic parameters were measured as described previously [9]. Briefly, rats were anesthetized with 2% halothane for instrumentation. For determination of the MBP and the central venous pressure (CVP), polyethylene catheters (PE-50; Imamura Co. Ltd, Tokyo, Japan) connected to a pressure transducer (P10EZ; Ohmeda, Singapore) were introduced into the right femoral artery and the superior vena cava through the right jugular vein, respectively. A catheter-tip transducer (Miller SPR 249; Miller Instruments, Houston, Tex., USA) was introduced into the left ventricle through the right carotid artery for the determination of the peak left ventricular pressure (LVP), the left ventricular end-diastolic pressure (LVEDP) and its first derivative ($\pm dP/dt$). After instrumentation the concentration of halothane was reduced to 0.5% and maintained for 20 min to record the steady-state hemodynamic parameters.

Echocardiographic Study

Two-dimensional echocardiography was performed in rats under 0.5% halothane anesthesia, using a 7.5-MHz transducer linked to an ultrasound system (SSD-5500; Aloka, Tokyo, Japan). M-mode images were obtained from the epicardial surface of the right ventricle, and short axis view of the left ventricle was recorded to measure the left ventricular dimension in diastole (LVDd) and left ventricular dimension in systole (LVDs). Left ventricular fractional shortening (FS) was calculated as diastolic dimension minus systolic dimension divided by diastolic dimension, expressed as percentage.

Histopathology

After echocardiographic measurement, hearts were removed and cleaned of the surrounding tissues. The heart weight (HW) was measured immediately, and the ratio of HW to body weight (H/B) was calculated. For the specimens stained with Azan-Mallory at the middle level of both ventricles, the area of myocardial fibrosis was quantified with a color image analyzer (CIA-102; Olympus, Tokyo, Japan), making use of differences in color (blue fibrotic area as opposed to red myocardium). The results were presented as the ratio of the fibrotic area to the area of myocardium [9].